GRAVITATIONAL INSTABILITY IN A PRIMORDIAL COLLAPSING GAS CLOUD

ABSTRACT

I. INTRODUCTION

An important problem in astrophysics is the study of the growth of small-scale fluctuations in the density and velocity inside a fluid body which is itself undergoing gravitational collapse. This is important for understanding the fragmentation of a cloud into gravitationally bound subunits, for instance in the problem of star formation inside a larger gas cloud, or the formation of substructure such as stars or star clusters inside a collapsing protogalaxy. One would like to know whether, given some initial level of fluctuations, it is possible for fragmentation to occur at all during the collapse, where we interpret fragmentation to mean the attainment of order unity fluctuations in the density, and, if so, what are the morphologies and preferred mass scales of the fragments. This subject has been reviewed in the context of star formation by, for instance, Tohline (1982). The development of fluctuations during collapse is also important in the study of dynamical relaxation of collisionless systems, where the growth of peculiar velocities on small scales is at least partially responsible for the phenomenon of "violent relaxation" (Lynden-Bell 1967). These ideas have recently been applied by Ryden and Gunn (1987) to the formation of galaxy halos by secondary infall, and by Aarseth, Lin, and Papaloizou (1988) to the collapse of protoglobular clusters.

Previous studies of this problem have been restricted either to background collapses having *uniform* density or to situations where *both* the background flow and the perturbations have some special (generally spherical) symmetry. The best understood case is where the background flow is both uniform and isotropic: Lifschitz (1946) first analyzed perturbations in a homogeneous isotropic cosmological model, while Hunter (1962, 1964) investigated perturbations in a uniform density collapsing spherical cloud. These flows have the common feature that the local velocity field expanded around any point comoving with the fluid is isotropic, as is the tidal component of the gravitational field, so that the latter depends only on the local mass density, and there are no tidal forces due to distant matter. Therefore the dynamics of the background flow are determined entirely locally, and the local velocity field is closely coupled to the local density throughout the collapse. These features are, however, not at all typical of a generic collapse, which tends to be both inhomogeneous and nonspherical—inhomogeneous because any slight degree of central concentration in the initial density causes the central parts to collapse on a shorter time scale than the outer parts, which increases the degree of central concentration; nonspherical because any slight degree of flattening initially present also tends to be amplified so long as the collapsing body is roughly homogeneous and the pressure is small (Lin, Mestel, and Shu 1965; Goodman and Binney 1983). In either case, the local gravitational field develops an anisotropic, tidal component, which in turn causes the local velocity field to become anisotropic, and to become decoupled from the local density. This can radically alter the evolution of perturbations, as compared to the homogeneous isotropic case. Work on perturbation behavior in such cases has been fairly restricted. Perturbations in inhomogeneous spherical collapses have been analyzed by McNally and Settle (1980), Ryden and Gunn (1987), and Silk and Suto (1988), but only for perturbations which are spherically symmetric. Perturbation evolution in the nonspherical collapse of a uniform density spheroid has been investigated by Falle (1972) and Silk (1982). In addition, there have been some calculations by Arny (1966, 1967) using an approximate particle method.

The purpose of this paper is to extend these previous analyses to more general background flows and perturbation geometries, in order to gain a better understanding of the effects of large-scale density gradients and anisotropic velocity fields on perturbation growth. The fundamental simplifying assumption made is to restrict the analysis to perturbations having wavelengths which are small compared to the characteristic scale of the background flow. I consider flows of collisional fluids in which the only forces acting are gravity and pressure, and in which the pressure depends only on the density, which excludes from consideration thermal and convective instabilities. The analysis for the case of zero pressure also applies to a collisionless fluid having negligible velocity dispersion, provided particle trajectories do not cross. In § II, I derive local evolution equations for perturbations to an arbitrary flow, in the linear regime and the short-wavelength limit. Local perturbation behavior in an inhomogeneous flow is found to be the same as that in a homogeneous anisotropic flow having the same local velocity field, this equivalent homogeneous flow being described by a matrix of scale factors $A_{ij}(t)$. In this paper I make the further assumption that the background flow is a pure shear flow, having zero vorticity. (The effects of rotation will be investigated in a future paper.) This allows some simplification of the perturbation equations; in particular, one can separate out the effects of perturbations in the vorticity (which need not be zero). In § III, I consider background flows in which the scale factors vary as power laws in time. This case provides a simple illustration of the relative effects of self-gravity, pressure, and kinematics of the background flow on the evolution of density perturbations. Sections IV and V present perturbation analyses for more realistic background flows. In order to have an analytical solution to perturb around, it is necessary to make some further simplifying assumptions; here I assume that the background flow has either spherical symmetry (§ IV) or planar symmetry (§ V), and that it is governed by gravity alone. The specific background flows considered, which are inhomogeneous, arise from the evolution into the non-linear regime of initially small density perturbations in an isotropically expanding cosmological model, as might be appropriate if the collapsing cloud represents a protogalaxy, for instance. However, similar results would be obtained for any other low-pressure background collapse having the same symmetry but different initial conditions, for instance, collapse from rest, as might be more appropriate for present-day star formation from gas clouds. The special symmetries assumed do not apply to the perturbations; further, the effects of pressure may be important for short-wavelength perturbations despite being unimportant on the scale of the background flow. Section VI compares the results obtained here with those of previous authors and tries to extract general qualitative features which should apply to a generic background flow. The most important result is that for low-pressure, inhomogeneous collapses, kinematic effects tend to come to dominate over self-gravity in driving perturbation growth as the collapse proceeds; this is in contrast to homogeneous, isotropic collapses, for which the effects of self-gravity and kinematics on perturbation growth are at all stages comparable. As a consequence, in a general flow, growth rates for plane wave perturbations develop a strong dependence on the direction of the wavevector, and the nonlinear evolution of perturbations is likely to take the form of collapse to planar structures or "pancakes." This idea motivates § VII, which is an analysis of perturbation evolution in a thin fluid sheet which is anisotropically expanding or contracting in its own plane. This is the two-dimensional analog of the three-dimensional analysis presented in the previous sections of the paper, but shows some distinct features, especially in relation to the effects of self-gravity. Section VIII summarizes the main results.

The analysis in this paper assumes that perturbations on small scales are in the linear regime of growth, while the larger scale background flow in which they are situated is in general nonlinear. As applied to galaxy formation, this analysis is therefore most applicable to "top-down" scenarios, in which large-scale structures collapse first and small-scale structures later. In this case, the development of structure on small scales is profoundly affected by that on large scales. On the other hand, in "bottom-up" or hierarchical scenarios, perturbations on small scales go nonlinear first, so the influence of large-scale perturbations on small-scale collapse is correspondingly weaker. Specifically, suppose that there is a spectrum of perturbations, such that the rms density fluctuation averaged over spherical regions of mass M has the dependence $\langle(\delta\rho/\rho)^2\rangle^{1/2} \propto M^\alpha$ over some mass range. Then for $\alpha = 0$, perturbations on all scales collapse simultaneously, while $\alpha > 0$ and $\alpha < 0$ correspond to top-down and bottom-up scenarios, respectively. The more negative α is, the weaker the effects of large scales on small scales. For the currently popular cold dark matter scenario (e.g., Blumenthal et al. 1984), the effective value of α is only slightly negative on galactic and subgalactic scales, so even though small-scale structures collapse first, one expects the influence on them of larger scale structure to be significant, although probably not as extreme as discussed in the body of this paper.

A matter of notation: in this paper, the symbol "$\sim$" is reserved for asymptotic equality, and "$\simeq$" for equality to order of magnitude.

II. GENERAL EQUATIONS

a) Fluid Equations

We consider a fluid flow with density ρ and velocity $\boldsymbol{u}$, with forces derived from a gravitational potential Φ and a pressure p. We assume a barotropic equation of state, $p = p(\rho)$, so that one can define an enthalpy $h(\rho) = \int dp/\rho = \int c_s^2 \, d\rho/\rho$, where $c_s = (dp/d\rho)^{1/2}$ is the sound speed. All buoyancy effects therefore vanish (see Balbus 1988b). The flow can be described in terms either of inertial coordinates $\boldsymbol{x}$, or in terms of coordinates $\boldsymbol{X}$ that comove with the fluid. We define the comoving coordinates such that $\boldsymbol{X} = \boldsymbol{x}$ at some initial time $t = t_i$. The equations of motion in inertial coordinates are

$$\frac{D\rho}{Dt} = -\rho \nabla_x \cdot \boldsymbol{u} , \qquad (2.1)$$

$$\frac{D\boldsymbol{u}}{Dt} = -\nabla_x \Phi - \frac{\nabla_x p}{\rho} = -\nabla_x(\Phi + h) \equiv -\nabla_x \Psi , \qquad (2.2)$$

$$\nabla_x^2 \Phi = 4\pi G\rho , \qquad (2.3)$$

where

$$\frac{D}{Dt} \equiv \left.\frac{\partial}{\partial t}\right|_x + \boldsymbol{u} \cdot \nabla_x = \left.\frac{\partial}{\partial t}\right|_X \qquad (2.4)$$

is the usual comoving derivative, and $\Psi = \Phi + h$ is the effective potential. The quantity ∇_x denotes the gradient operator

with respect to coordinates x, and $\partial/\partial t|_x$ the time derivative taken at constant x.

A consequence of the barotropic equation of state assumed is that Kelvin's circulation theorem applies to the flow. The differential form of this, an evolution equation for the vorticity $\boldsymbol{\omega} = \nabla_x \wedge \boldsymbol{u}$, can be derived by taking the curl of equation (2.2) and using the continuity equation (2.1):

$$\frac{D}{Dt}\left(\frac{\boldsymbol{\omega}}{\rho}\right) = \left(\frac{\boldsymbol{\omega}}{\rho}\right) \cdot \nabla_x \boldsymbol{u} . \qquad (2.5)$$

b) Local Behavior of Background Flow

We begin with a local analysis of the background flow in the neighborhood of a fluid particle having coordinates $X = X_0$, $x = x_0(t)$ (see Peebles 1980, § 22). We define new coordinates relative to this particle: $X' = X - X_0$, $x' = x - x_0(t)$. The trajectory of any fluid particle can be expressed as $x = x(X, t)$; expanding this around $X = X_0$, we obtain

$$x'_i = A_{ij}(t)X'_j + O(X'^2) \qquad (2.6a)$$

where

$$A_{ij}(t) \equiv \frac{\partial x_i}{\partial X_j}\bigg|_0 \qquad (2.6b)$$

and $A_{ij}(t_i) = \delta_{ij}$. In these expressions, the summation convention is assumed, so that repeated indices are summed over. We define $\boldsymbol{u}' = \boldsymbol{u} - \boldsymbol{u}_0(t)$, where $\boldsymbol{u} = D\boldsymbol{x}/Dt = (\partial \boldsymbol{x}/\partial t)|_X$ and $\boldsymbol{u}_0 = \dot{\boldsymbol{x}}_0(t)$. Differentiating equation (2.6a) then gives

$$u'_i = \dot{A}_{ij}(t)X'_j + O(X'^2) = H_{ij}(t)x'_j + O(x'^2) , \qquad (2.7a)$$

where

$$H_{ij}(t) \equiv \frac{\partial u_i}{\partial x_j}\bigg|_0 = \dot{A}_{ik} A_{kj}^{-1} . \qquad (2.7b)$$

The fluid density is given by $\rho(X, t) = \rho(X, t_i)/\text{Det}\,(\partial x_i/\partial X_j)$ (this is equivalent to eq. [2.1]). Expanding around $X = X_0$ gives

$$\rho = \rho_0(t) + O(X') , \qquad (2.8a)$$

where

$$\rho_0(t) \equiv \rho(X_0\, t_i)/|A| , \qquad (2.8b)$$

and $|A|$ is the determinant of A_{ij}. An equation of motion for $A_{ij}(t)$ can be derived by differentiating equation (2.2) with respect to X:

$$\ddot{A}_{ij} = -\frac{\partial^2 \Psi}{\partial x_i \partial x_k}\bigg|_0 A_{kj} , \qquad (2.9)$$

Equation (2.9), together with equations (2.8) and (2.3) evaluated at $x = x_0$, constrains the evolution of the expansion factors $A_{ij}(t)$, but in general does not suffice to determine them completely, even when given appropriate initial conditions: the A_{ij} determine the local density ρ_0, and ρ_0 determines $h_0 = h(\rho_0)$ and the trace of the tidal tensor $(\partial^2 \Phi/\partial x_i \partial x_j)_0$. However, $\ddot{A}_{ij}$ depends on the components of $(\partial^2 h/\partial x_i \partial x_j)_0$, determined by the spatial derivatives of ρ, and on the various components of $(\partial^2 \Phi/\partial x_i \partial x_j)_0$ independently. In general, the trace-free part of the tidal tensor depends on the distribution of matter distant from the point under consideration. Thus, the local behavior can be determined only after a global solution has been found. For the special case of a homogeneous flow with spherical

symmetry, for which $A_{ij}(t) = a(t)\delta_{ij}$, equation (2.9) reduces to the Friedmann equation familiar in cosmology, $\ddot{a}/a = -(4\pi/3)G\rho$, and the local evolution *is* determined entirely in terms of local quantities.

c) Evolution Equations for Perturbations in a Shear Flow

We consider perturbations with characteristic wavelength λ small compared to the scale L on which the background flow varies, $\lambda \ll L$. We also assume that the perturbations have small amplitude. Define perturbed quantities

$$\rho = \rho_b(1 + \epsilon) , \quad \boldsymbol{u}' = \boldsymbol{u}'_b + \boldsymbol{v} ,$$
$$\Psi = \Psi_b + \psi , \qquad \Phi = \Phi_b + \chi , \qquad (2.10)$$

The subscript b denotes the unperturbed background solution. These quantities are considered as functions of coordinates x' measured relative to the *unperturbed* position of the reference particle, or of coordinates X' comoving with the *unperturbed* flow. The expansions (2.7) and (2.8) now describe only the unperturbed quantities u'_b and ρ_b. Substituting the perturbed solution in equation (2.1), and subtracting off the unperturbed equation, one obtains

$$\frac{\partial(\rho_b \epsilon)}{\partial t}\bigg|_{x'} + \boldsymbol{u}'_b \cdot \nabla_{x'}(\rho_b \epsilon) =$$
$$-\rho_b \epsilon \nabla_{x'} \cdot \boldsymbol{u}'_b - \nabla_{x'} \cdot [\rho_b(1 + \epsilon)\boldsymbol{v}] . \quad (2.11)$$

The quantity on the left-hand side is a time derivative $\partial/\partial t|_x$ comoving with the unperturbed flow. Making use again of the unperturbed continuity equation, one derives

$$\frac{\partial \epsilon}{\partial t}\bigg|_{x'} = -\nabla_{x'} \cdot [(1 + \epsilon)\boldsymbol{v}] - (1 + \epsilon)\boldsymbol{v} \cdot \frac{\nabla_{x'}\rho_b}{\rho_b} . \quad (2.12)$$

The evolution of $\boldsymbol{u}'$ follows from $D\boldsymbol{u}'/Dt = D\boldsymbol{u}/Dt - \dot{\boldsymbol{u}}_0(t)$, with $D\boldsymbol{u}/Dt$ given by equation (2.2) and $\dot{\boldsymbol{u}}_0 = \nabla\Psi_b|_0$. Substituting the perturbed solution, and subtracting off the unperturbed equation, one obtains

$$\frac{\partial \boldsymbol{v}}{\partial t}\bigg|_{x'} + \boldsymbol{v} \cdot \nabla_{x'}(\boldsymbol{u}'_b + \boldsymbol{v}) = -\nabla_{x'}\psi , \qquad (2.13)$$

Equation (2.3) gives for the perturbed gravitational potential

$$\nabla^2_{x'}\chi = 4\pi G\rho_b \epsilon . \qquad (2.14)$$

The preceding equations for the perturbation are exact. We now make two simplifying approximations: we assume that the perturbation amplitude is small, so that terms which are quadratic in the perturbation can be discarded. We also assume that distances and wavelengths are small compared to the background scale, $x'/L \ll 1$, $\lambda/L \ll 1$, so that terms of order x'/L, λ/L can be neglected. Substituting the expansions (2.6), (2.7), and (2.8) for x', u'_b, and ρ_b in terms of X' into equations (2.12), (2.13) and (2.14) respectively, one obtains

$$\frac{\partial \epsilon}{\partial t}\bigg|_{x'} = -A_{ji}^{-1}\frac{\partial v_i}{\partial X'_j} , \qquad (2.15)$$

$$\frac{\partial v_i}{\partial t}\bigg|_{x'} + H_{ij}v_j = -A_{ji}^{-1}\frac{\partial \psi}{\partial X'_j} , \qquad (2.16)$$

$$A_{ji}^{-1}A_{ki}^{-1}\frac{\partial^2 \chi}{\partial X'_j \partial X'_k} = 4\pi G\rho_0 \epsilon . \qquad (2.17)$$

With the same approximations, the perturbation in the enth-

alpy is $\delta h = c_s^2 \epsilon$, with $c_s(\rho)$ evaluated at $\rho = \rho_0 \equiv \rho_{b0}$. Thus the perturbation in the effective potential is

$$\psi = \chi + c_s^2 \epsilon \,. \qquad (2.18)$$

The effect of the short-wavelength assumption is thus to reduce the perturbation equations to the same form as they would have in a homogeneous background flow having the same scale factors $A_{ij}(t)$ and density $\rho_0(t)$ at all points. In such a flow, the velocity law $u'_{bi} = H_{ij} x'_j$ would be exact. The inhomogeneity of the true background flow thus enters only through the effect it has on the behavior of the scale factors $A_{ij}(t)$.

The preceding equations are valid for an arbitrary background flow. We now specialize to a background flow having zero vorticity ($\nabla_x \wedge \boldsymbol{u}_b = 0$), i.e., *a pure shear flow*. For such a flow, $H_{ij} = H_{ji}$, and the perturbation equations can be simplified by defining a new velocity variable, the "peculiar momentum" $\boldsymbol{V}$:

$$V_i \equiv A_{ji} v_j \,. \qquad (2.19)$$

Substituting this definition and equation (2.18) for ψ in equation (2.16), and using the definition (2.7b) for H_{ij}, we obtain

$$\left. \frac{\partial \boldsymbol{V}}{\partial t} \right|_{x'} = -\nabla_{x'}(\chi + c_s^2 \epsilon) \,. \qquad (2.20)$$

We see that if the perturbed force were zero, $\boldsymbol{V}$ would be constant with time, $\boldsymbol{V} = \boldsymbol{V}(X')$. Another useful result that can be derived from equation (2.20) concerns vorticity. Define "comoving vorticity" by $\boldsymbol{\Omega} = \nabla_{X'} \wedge \boldsymbol{V}$. Taking the curl of equation (2.20) gives

$$\left. \frac{\partial \boldsymbol{\Omega}}{\partial t} \right|_{x'} = 0 \,, \qquad (2.21)$$

from which follows $\boldsymbol{\Omega} = \boldsymbol{\Omega}(X')$. This result could alternatively be derived from the vorticity equation (2.5), noting that the vorticity of the background flow is zero. The components of $\boldsymbol{\omega}$ and $\boldsymbol{\Omega}$ are related by $\Omega_i = |A| A_{ij}^{-1} \omega_j$.

d) Plane Wave Perturbations in a Shear Flow

Fourier transforming the linearized perturbation equations with respect to X', one finds that the different Fourier components of the perturbation evolve independently. Therefore an arbitrary solution can be represented as a superposition of plane waves, each having spatial dependence of the form $\exp(i\boldsymbol{q} \cdot \boldsymbol{X'}) = \exp(i\boldsymbol{k} \cdot \boldsymbol{x'})$. For a single plane wave, we have

$$\epsilon(X', t) = \epsilon(t) \exp(i\boldsymbol{q} \cdot \boldsymbol{X'}) \,,$$
$$V(X', t) = V(t) \exp(i\boldsymbol{q} \cdot \boldsymbol{X'}) \,, \qquad (2.22)$$
$$\chi(X', t) = \chi(t) \exp(i\boldsymbol{q} \cdot \boldsymbol{X'}) \,.$$

We use the same symbol for a quantity and for its Fourier amplitude, since it should be clear from the context which is meant. The *comoving* wavevector $\boldsymbol{q}$ has components which are constant with time, while the *proper* wavevector $\boldsymbol{k}$ evolves in time as the wave is sheared by the background flow:

$$k_i(t) = A_{ji}^{-1}(t) q_j \,. \qquad (2.23)$$

Substituting equation (2.22) in equations (2.15), (2.20), and (2.17), respectively, one obtains

$$\frac{d\epsilon}{dt} = -i A_{ji}^{-1} A_{ki}^{-1} q_j V_k \,, \qquad (2.24)$$

$$\frac{dV}{dt} = -i\boldsymbol{q}(\chi + c_s^2 \epsilon) \,, \qquad (2.25)$$

$$\chi = -\frac{4\pi G \rho_0 \epsilon}{A_{ji}^{-1} A_{ki}^{-1} q_j q_k} \,. \qquad (2.26)$$

It is convenient to decompose $\boldsymbol{V}$ into components parallel and perpendicular to $\boldsymbol{q}$:

$$\boldsymbol{V} = V_\parallel \hat{\boldsymbol{q}} + \boldsymbol{V}_\perp \,, \qquad (2.27a)$$

where

$$V_\parallel = \hat{\boldsymbol{q}} \cdot \boldsymbol{V} \,, \quad \boldsymbol{q} \cdot \boldsymbol{V}_\perp = 0 \,, \qquad (2.27b)$$

and $\hat{\boldsymbol{q}} = \boldsymbol{q}/q$. Vorticity conservation (eq. [2.21]) gives $\boldsymbol{\Omega} = i\boldsymbol{q} \wedge \boldsymbol{V} = \text{constant}$; thus

$$\boldsymbol{V}_\perp = \text{constant} \,. \qquad (2.28)$$

Substituting equation (2.27) into equation (2.24) gives an evolution equation for ϵ:

$$\frac{d\epsilon}{dt} = -i P_{ij} q_i \left(q_j \frac{V_\parallel}{q} + V_{\perp j} \right) \,, \qquad (2.29)$$

and substituting equations (2.26) and (2.27) into equation (2.25) gives an evolution equation for $V_\parallel$:

$$\frac{dV_\parallel}{dt} = iq \left(\frac{4\pi G \rho_0}{P_{ij} q_i q_j} - c_s^2 \right) \epsilon \,. \qquad (2.30)$$

We have defined

$$P_{ij}(t) \equiv A_{ik}^{-1}(t) A_{jk}^{-1}(t) \,. \qquad (2.31)$$

Eliminating $V_\parallel$ between equations (2.29) and (2.30), one obtains a single equation for the relative density perturbation ϵ:

$$\frac{d^2\epsilon}{dt^2} - \left(\frac{\dot{P}_{ij} q_i q_j}{P_{kl} q_k q_l} \right) \frac{d\epsilon}{dt} + (c_s^2 P_{ij} q_i q_j - 4\pi G \rho_0) \epsilon$$
$$= -i \left[\dot{P}_{ij} - \left(\frac{\dot{P}_{kl} q_k q_l}{P_{mn} q_m q_n} \right) P_{ij} \right] q_i V_{\perp j} \,. \qquad (2.32a)$$

Noting that $k^2 = k_i k_i = P_{jk} q_j q_k$ allows us to rewrite this as

$$\frac{d^2\epsilon}{dt^2} - 2 \frac{\dot{k}}{k} \frac{d\epsilon}{dt} + (c_s^2 k^2 - 4\pi G \rho_0) \epsilon = -i \left(\dot{P}_{ij} - 2 \frac{\dot{k}}{k} P_{ij} \right) q_i V_{\perp j} \,. \qquad (2.32b)$$

e) Shear Flow with Fixed Principal Axes

A shear flow is particularly simple if the principal axes of the shear are fixed in inertial space. The flows analyzed in later sections of this paper all have this property. In this case, the matrix A_{ij} is diagonal in the nonrotating coordinate system defined by the principal axes, so we can write

$$A_{ij} = \text{diag}(a_1, a_2, a_3) \,, \qquad V = (a_1 v_1, a_2 v_2, a_3 v_3) \,,$$
$$k = (q_1/a_1, q_2/a_2, q_3/a_3) \,, \quad P_{ij} = \text{diag}(1/a_1^2, 1/a_2^2, 1/a_3^2) \,. \qquad (2.33)$$

Hereafter the summation convention will *not* apply, and all summations will be indicated explicitly. The evolution equation (2.32a) for ϵ reduces to

$$\frac{d^2\epsilon}{dt^2} + 2 \left[\frac{\sum_i (q_i/a_i)^2 (\dot{a}_i/a_i)}{\sum_i (q_i/a_i)^2} \right] \frac{d\epsilon}{dt} + \left[c_s^2 \sum_i \left(\frac{q_i}{a_i} \right)^2 - 4\pi G \rho_0 \right] \epsilon$$
$$= 2i \left\{ \sum_i \frac{q_i V_{\perp i} \dot{a}_i}{a_i^3} - \left[\frac{\sum_i (q_i/a_i)^2 (\dot{a}_i/a_i)}{\sum_i (q_i/a_i)^2} \right] \sum_i \frac{q_i V_{\perp i}}{a_i^2} \right\} \,. \qquad (2.34)$$

We notice several things from the above equation (similar remarks can be made about the more general equations [2.32a] or [2.32b]): (1) The effects of the perturbed gravity and perturbed pressure are contained entirely in a term $(4\pi G\rho_0 - c_s^2 k^2)\epsilon$. The effects of gravity and pressure exactly balance at the Jeans wavenumber $k_J \equiv (4\pi G\rho_0)^{1/2}/c_s$. This is the same result as one derives for perturbations in a static medium. For $k < k_J$, gravity dominates, and this term tends to drive growth of ϵ; for $k > k_J$, pressure dominates and tends to drive oscillations of ϵ (i.e., sound waves). (2) The expansion/contraction of the background flow results in the appearance in equation (2.34) of a $d\epsilon/dt$ term with coefficient depending on $\dot{a}_i/a_i$, as in the analysis of perturbations to a homogeneous isotropic cosmological model (e.g., Weinberg, 1972, § 15.9), although the coefficient has a more complicated form because the expansion factors are different along different directions. In the cosmological case, one considers an expanding background ($\dot{a}_i/a_i > 0$), so that this term tends to cause decay of ϵ, but for a background flow which is collapsing ($\dot{a}_i/a_i < 0$), this term can drive a *growth* of ϵ. This turns out to be an important effect, as we will see later. (3) *Unlike* the homogeneous isotropic case, perturbations in vorticity ($V_\perp \neq 0$) in general drive perturbations in density, and hence also perturbations in $V_\parallel$ (eq. [2.30]). Physically, this density growth occurs because even if k and v are initially perpendicular, both vectors are sheared toward the principal axis having the largest expansion factor, so that $\nabla_x \cdot v = ik \cdot v$ develops a nonzero value. Thus, a perturbation which initially has V perpendicular to q develops a component of V parallel to q. The converse is not true; if V is initially parallel to q, then V remains parallel to q, and v remains parallel to k, as a result of vorticity conservation. Thus, there are pure density perturbations ($\epsilon \neq 0$, $V_\perp = 0$), but in general no pure vorticity perturbations ($\epsilon = 0$, $V_\perp \neq 0$).

The analysis simplifies further if we consider perturbations having wavevector parallel to one of the principal axes. Suppose $q = (q_1, 0, 0)$ so that $k = (k_1/a_1, 0, 0)$. Then equation (2.34) reduces to

$$\frac{d^2\epsilon}{dt^2} + 2\frac{\dot{a}_1}{a_1}\frac{d\epsilon}{dt} + \left[c_s^2\left(\frac{q_1}{a_1}\right)^2 - 4\pi G\rho_0\right]\epsilon = 0 . \quad (2.35)$$

Notice that the vorticity term has disappeared, so that for this special case, vorticity perturbations completely decouple from density perturbations. The evolution is controlled by the competition between the kinematic term $2(\dot{a}_1/a_1)d\epsilon/dt$, the pressure term $c_s^2(q_1/a_1)^2\epsilon$, and the self-gravity term $-4\pi G\rho_0\epsilon$. The above equation is exactly the same as one derived for an isotropic cosmological model having expansion factor $a_1(t)$. This is not surprising, because if the expansion is isotropic, any direction may be taken as the principal direction. Equation (2.35), in fact, has wider applicability than it might at first appear. At the initial time, the scale factors are all equal, by definition. Suppose that as the evolution proceeds, one of the scale factors, say a_1, becomes much smaller than the other two. Then, for generic q and $V_\perp$, the proper wavevector tends to align with the 1-axis, $k \approx (q_1/a_1, 0, 0)$, and the $i = 1$ term tends to dominate in the various sums $\sum_i$ in equation (2.34). In this limit, equation (2.34) approaches the form (2.35), and the form of the density evolution becomes independent of whether or not the perturbation has vorticity.

III. POWER-LAW SCALE FACTORS

In this section, we consider the evolution of perturbations when the principal axes are fixed, $A_{ij}(t) = \mathrm{diag}\,(a_1, a_2, a_3)$, and

the scale factors have a power-law dependence on time: $a_i(t) \propto |t - t_c|^{\alpha_i}$. This case serves to demonstrate some general qualitative features in a simple way, and also correctly describes the limiting behaviors (as $t \rightarrow t_c$) in certain more realistic background solutions. We mainly have in mind the case that the background flow represents a collapse, so that at least one of the a_i has the behavior $a_i \rightarrow 0$ as $t \rightarrow t_c$, but the analysis will apply equally well to the case of expansion from an initial singularity.

The scale factors are normalized to unity at time $t_i: a_i(t_i) = 1$. The equation of state is assumed to be of the form $p \propto \rho^\gamma$, so that the sound speed has the dependence $c_s^2 \propto \rho^{\gamma-1}$. The astrophysically interesting range for γ is $1 \leq \gamma \leq 5/3$. It is convenient to define a dimensionless time variable $\tau \equiv (4\pi G\rho_i)^{1/2}|t - t_c|$, where $\rho_i \equiv \rho(t_i)$. Substituting these definitions into equation (2.35) for the evolution of a density perturbation with $q = (q_1, 0, 0)$, we derive

$$\frac{d^2\epsilon}{d\tau^2} + 2\left(\frac{da_1/d\tau}{a_1}\right)\frac{d\epsilon}{d\tau} - \frac{\rho}{\rho_i}\left[1 - \left(\frac{\rho}{\rho_i}\right)^{\gamma-2}\frac{(q_1/q_{1Ji})^2}{a_1^2}\right]\epsilon = 0 . \quad (3.1)$$

We have defined a comoving Jeans wavenumber along the 1-axis:

$$q_{1J}(t) \equiv a_1 k_J = \frac{(4\pi G\rho)^{1/2}}{c_s}a_1$$

$$= \frac{(4\pi G\rho_i)^{1/2}}{c_{si}}\left(\frac{\rho}{\rho_i}\right)^{(2-\gamma)/2}a_1 \equiv q_{1Ji}\left(\frac{\rho}{\rho_i}\right)^{(2-\gamma)/2}a_1 , \quad (3.2)$$

so that the factor in brackets in equation (3.1) may be written $[1 - (q_1/q_{1J})^2]$. Note that $q_{1Ji} = k_{Ji}$. We now assume that the scale factors have the dependence $a_i(\tau) = (\tau/\tau_i)^{\alpha_i}$. Define $\beta \equiv \alpha_1 + \alpha_2 + \alpha_3$, then $\rho/\rho_i = 1/a_1a_2a_3 = (\tau/\tau_i)^{-\beta}$. (We assume $\beta > 0$.) Equation (3.1) becomes

$$\frac{d^2\epsilon}{d\tau^2} + \frac{2\alpha_1}{\tau}\frac{d\epsilon}{d\tau} - \left(\frac{\tau}{\tau_i}\right)^{-\beta}\left[1 - \left(\frac{q_1}{q_{1Ji}}\right)^2\left(\frac{\tau}{\tau_i}\right)^{(2-\gamma)\beta - 2\alpha_1}\right]\epsilon = 0 . \quad (3.3)$$

We now examine the limiting behavior of the solutions of equation (3.3) as $\tau \rightarrow 0$. This depends on the behavior of the comoving Jeans wavenumber $q_{1J}(\tau) = q_{1Ji}(\tau/\tau_i)^{[(\gamma-2)\beta + 2\alpha_1]/2}$. If $(\gamma - 2)\beta + 2\alpha_1 < 0$, i.e., $\gamma < 2(1 - \alpha_1/\beta) = 2(\alpha_1 + \alpha_2)/(\alpha_1 + \alpha_2 + \alpha_3)$, then $q_{1J} \rightarrow \infty$ as $\tau \rightarrow 0$, so that for any initial wavenumber q_1, the self-gravity of the perturbation eventually comes to dominate over its pressure. In the opposite case, $(\gamma - 2)\beta + 2\alpha_1 > 0$, $q_{1J} \rightarrow 0$ as $\tau \rightarrow 0$, so that pressure eventually dominates self-gravity. We consider these cases in turn. (The results for the special case $(\gamma - 2)\beta + 2\alpha_1 = 0$ do not differ essentially from the other two cases, so we do not list them here.)

a) $(\gamma - 2)\beta + 2\alpha_1 < 0$

In this case, $q_1/q_{1J} \rightarrow 0$ as $\tau \rightarrow 0$, so in this limit, equation (3.3) approximates to

$$\frac{d^2\epsilon}{d\tau^2} + \frac{2\alpha_1}{\tau}\frac{d\epsilon}{d\tau} - \frac{B\epsilon}{\tau^\beta} = 0 , \quad (3.4)$$

where $B = \tau_i^\beta$. (Alternatively, if the pressure is identically zero, this is valid for all τ.) The leading order behavior as $\tau \rightarrow 0$ of the solutions to equation (3.4) may be found by standard methods (e.g., Bender and Orszag 1978, chapt. [3]). There are several cases.

i) $\beta < 2$

The ϵ/τ^β term becomes negligible compared to the others as $\tau \to 0$, assuming that $\alpha_1 \neq 0$. The independent solutions have the form

$$\epsilon \sim c_1 \tau^{1-2\alpha_1} , \quad \epsilon \sim c_2 . \tag{3.5}$$

ii) $\beta = 2$

Equation (3.4) has exact solutions of the form

$$\epsilon = c_1 \tau^{p^+} , \quad \epsilon = c_2 \tau^{p^-} , \tag{3.6a}$$

where

$$p_\pm = \tfrac{1}{2}[(1 - 2\alpha_1) \pm \sqrt{(1 - 2\alpha_1)^2 + 4B}] . \tag{3.6b}$$

The roots $p_\pm$ are always real.

iii) $\beta > 2$

The rapid divergence of the ϵ/τ^β term as $\tau \to 0$ results in solutions having WKB–like behavior:

$$\epsilon \sim c_\pm \tau^{-(\alpha_1 - \beta/4)} \exp\left[\pm \frac{B^{1/2}\tau^{-(\beta/2-1)}}{(\beta/2 - 1)} \right] . \tag{3.7}$$

However, this case seems unlikely to occur in practice: it requires the local density to diverge faster than $\rho \propto (t_c - t)^{-2}$ as $t \to t_c$.

b) $(\gamma - 2)\beta + 2\alpha_1 > 0$

In this case, $q_1/q_{1J} \to \infty$ as $\tau \to 0$, so in this limit, equation (3.3) approximates to

$$\frac{d^2\epsilon}{d\tau^2} + \frac{2\alpha_1}{\tau} \frac{d\epsilon}{d\tau} + \frac{D\epsilon}{\tau^{\delta_1}} = 0 , \tag{3.8}$$

where we have defined $\delta_1 = (\gamma - 1)\beta + 2\alpha_1$, $D = (q_1/q_{1Ji})^2 \tau_i^{\delta_1}$. The leading order behaviors in the various cases are as follows,

i) $\delta_1 < 2$

The ϵ/τ^{δ_1} term becomes negligible compared to the others as $\tau \to 0$, for $\alpha_1 \neq 0$, so that this case is equivalent to case (a[i]), the solutions being

$$\epsilon \sim c_1 \tau^{1-2\alpha_1} , \quad \epsilon \sim c_2 . \tag{3.9}$$

ii) $\delta_1 = 2$

Equation (3.8) has exact solutions

$$\epsilon = c_1 \tau^{p^+} , \quad \epsilon = c_2 \tau^{p^-} , \tag{3.10a}$$

where

$$p_\pm = \tfrac{1}{2}[(1 - 2\alpha_1) \pm \sqrt{(1 - 2\alpha_1)^2 - 4D}] . \tag{3.10b}$$

The roots $p_\pm$ are real for $D < \tfrac{1}{4}(1 - 2\alpha_1)^2$, and complex for $D > \tfrac{1}{4}(1 - 2\alpha_1)^2$.

iii) $\delta_1 > 2$

The rapid divergence of the ϵ/τ^{δ_1} term results in solutions with WKB–like behavior:

$$\epsilon \sim c_\pm \tau^{-(\alpha_1 - \delta_1/4)} \exp\left[\pm i \frac{D^{1/2}\tau^{-(\delta_1/2-1)}}{(\delta_1/2 - 1)} \right] . \tag{3.11}$$

The competition between the kinematic, self-gravity, and pressure terms in equation (3.3) thus results in the following behavior for ϵ as $\tau \to 0$. In cases (a[i]) and (b[i]), the kinematic term dominates over the other two. The solutions are of power-law form. One solution is constant, and the other is growing (as $\tau \to 0$) if $\alpha_1 > \tfrac{1}{2}$, and decaying if $\alpha_1 < \tfrac{1}{2}$. Thus,

growing solutions are possible even if $k > k_J$, so that pressure dominates over self-gravity. In case (a[iii]), the self-gravity term dominates, and there are growing and decaying solutions dominated by an exponential of a power of τ which grows as $\tau \to 0$. These solutions are WKB modifications of the solutions $\epsilon \propto \exp[\pm (4\pi G\rho)^{1/2}t]$ which arise in the static Jeans problem for $k \ll k_J$. The expansion/contraction of the background has the effect of making the growth rate $(4\pi G\rho)^{1/2}$ a function of time, resulting in the somewhat more complicated form (3.7) (see Zel'dovich and Novikov 1983, chapt. [10]). In case (b[iii]), the pressure term dominates, and the solutions are oscillatory in time. The phase of the oscillation grows as a power of τ as $\tau \to 0$. These solutions are the WKB modifications of the solutions $\epsilon \propto \exp(\pm ikc_s t)$ which arise in the static Jeans problem for $k \gg k_J$. The expansion/contraction of the background flow makes the wavenumber and sound speed functions of time, so that the phase is no longer linear in t. The expansion also causes the amplitude of the oscillation to vary with time. The solution (3.11) has amplitude increasing as $\tau \to 0$ if $\alpha_1 > \delta_1/4$.

IV. SPHERICAL BACKGROUND FLOW

a) Background Flow

In this section, we consider perturbations in a background flow which has spherical symmetry. The gravitational field is assumed to arise solely from the fluid itself. To simplify the analysis, we assume that the effects of pressure may be neglected on the scale of the background flow, and that the orbits of spherical mass shells do not cross. Formally, we continue the analysis up to when a shell has collapsed to zero radius. In practice, one or other of the preceding assumptions may break down before this point is reached. If the fluid is collisionless, then spherical shells can reexpand after collapsing to zero radius, passing through other infalling shells. If the fluid is collisional, and the equation of state is stiff enough (barotropic exponent $\gamma > 4/3$), then the pressure will eventually build up to a large enough value at the center to halt the collapse there, even if the pressure is very small initially (Zel'dovich and Kazhdan 1970). This may involve formation of a shock front at the junction between freely infalling matter and a pressure supported core. The analysis which follows is valid only up to the point when shell crossing or pressure become important.

For a spherical flow, the fluid velocity is radial, so that the principal axes at any comoving point are fixed in time, and are aligned along the outward radial (r) direction and along two perpendicular tangential (t) directions, all tangential directions being equivalent. Thus, $A_{ij}(t) = \mathrm{diag}\,(a, b, b)$ where $a \equiv a_r$, $b \equiv a_t$. We can write the radius of a spherical shell as $r = (r_i, t)$, where r_i is the radius at time t_i. Then the scale factors are given by equations (2.6b) as

$$b(r_i, t) = \frac{r(r_i, t)}{r_i} , \tag{4.1a}$$

$$a(r_i, t) = \frac{\partial r}{\partial r_i}\bigg|_t = b + r_i \frac{\partial b}{\partial r_i}\bigg|_t . \tag{4.1b}$$

The equations of motion for a and b may be derived either from equation (2.9) with $\Phi = \Phi(r, t)$ and $h = 0$, or from equation (4.1) and the equation of motion for $r(r_i, t)$. Defining $M(r, t)$ to be the total mass within radius r and $\bar\rho(r, t) =$

$M(r, t)/(4\pi r^3/3)$ the mean density within radius r, we have

$$\frac{\ddot{b}}{b} = -\frac{GM}{r^3} = -\frac{4\pi}{3}G\bar{\rho} , \qquad (4.2a)$$

$$\frac{\ddot{a}}{a} = -4\pi G\rho + \frac{2GM}{r^3} = -\frac{4\pi}{3}G(3\rho - 2\bar{\rho}) , \qquad (4.2b)$$

where $\ddot{b} \equiv \partial b/\partial t|_{r_i}$, etc. Clearly, $\ddot{b}/b < 0$ always, so that gravitational forces tend to cause compression in the tangential direction, but $\ddot{a}/a$ may have either sign. For a density distribution that monotonically decreases with radius, $d\rho/dr \leq 0$, $\rho \leq \bar{\rho}$, so that $\ddot{a}/a \geq \ddot{b}/b$, and radial separations tend to be stretched relative to tangential separations. The extreme cases are a homogeneous density distribution, for which $\rho = \bar{\rho}$, and $\ddot{a}/a = \ddot{b}/b < 0$, and a very centrally concentrated mass distribution, for which $\rho/\bar{\rho} \to 0$, and $\ddot{a}/a = -2\ddot{b}/b > 0$.

Assuming that there is no shell crossing, the total mass inside any comoving spherical shell is constant, so that the time dependence of ρ and $\bar{\rho}$ at fixed r_i is $\rho = \rho_i/ab^2$, $\bar{\rho} = \bar{\rho}_i/b^3$, where $\rho_i(r_i) = \rho(r_i, t_i)$, etc. It is convenient to define a dimensionless time-variable for each spherical shell

$$\tau(r_i, t) \equiv (4\pi G\bar{\rho}_i/3)^{1/2}t . \qquad (4.3)$$

Equations (4.2a) and (4.2b) then become

$$\left.\frac{\partial^2 b}{\partial\tau^2}\right|_{r_i} = -\frac{1}{b^2} , \qquad (4.4a)$$

$$\left.\frac{\partial^2 a}{\partial\tau^2}\right|_{r_i} = -3\frac{(\rho_i/\bar{\rho}_i)}{b^2} + 2\frac{a}{b^3} , \qquad (4.4b)$$

Equation (4.4a) for $b(r_i, \tau)$ has a first integral

$$\frac{1}{2}\left(\frac{\partial b}{\partial\tau}\right)^2 - \frac{1}{b} = \frac{1}{2}\left(\frac{\partial b}{\partial\tau}\right)_i^2 - 1 \equiv -\frac{1}{b_m} , \qquad (4.5)$$

partial derivatives being taken at constant r_i. We assume that all shells are gravitationally bound, so that $b_m(r_i) > 0$. Then equation (4.5) has the parametric solution

$$b(r_i, \theta) = \left(\frac{b_m}{2}\right)(1 - \cos\theta) , \qquad (4.6a)$$

$$\tau(r_i, \theta) - \tau_i(r_i) = \left(\frac{b_m}{2}\right)^{1/2}[\theta - \sin\theta - (\theta_i - \sin\theta_i)] , \qquad (4.6b)$$

where $\tau_i(r_i) = \tau(r_i, t_i)$, and

$$\theta_i = \begin{cases} 2\sin^{-1}(1/\sqrt{b_m}) , & (\partial b/\partial\tau)_i > 0 , \\ 2\pi - 2\sin^{-1}(1/\sqrt{b_m}) , & (\partial b/d\tau)_i < 0 , \end{cases} \qquad (4.6c)$$

where $\sin^{-1} x$ denotes the principal value. Combined with equation (4.3), equation (4.6) gives $b(r_i, t)$. The evolution of the tangential scale factor b for fixed r_i depends on the initial conditions only through $\bar{\rho}_i(r_i)$ and $(\partial b/\partial t)_i = (\dot{r}/r)|_{r=r_i, t=t_i}$. With $b(r_i, t)$ known, the solution for $a(r_i, t)$ could be determined using equation (4.4b), but it is simpler to differentiate the solution for b and use the second form of equation (4.1b). Expanding the derivative gives

$$a = b + \frac{r_i}{(\partial\tau/\partial\theta)|_{r_i}}\left[\left.\frac{\partial b}{\partial r_i}\right|_\theta\left.\frac{\partial\tau}{\partial\theta}\right|_{r_i} + \left.\frac{\partial b}{\partial\theta}\right|_{r_i}\left(\left.\frac{\partial\tau}{\partial r_i}\right|_t - \left.\frac{\partial\tau}{\partial r_i}\right|_\theta\right)\right] . \qquad (4.7)$$

Substituting in the parametric solution for b, together with the

definitions of $\tau(r_i, t)$, $\theta_i(r_i)$, and $b_m(r_i)$, one obtains

$$a(r_i, \theta) = b(r_i, \theta) + \left[\frac{\partial\ln(\partial b/\partial t)_i}{\partial\ln r_i}\right]f(\theta, \theta_i) + \left(\frac{\partial\ln\bar{\rho}_i}{\partial\ln r_i}\right)g(\theta, \theta_i) , \qquad (4.8a)$$

where

$$f(\theta, \theta_i) = \frac{1}{2}b_m\left(\frac{\sin\theta}{1 - \cos\theta}\right)(b_m - 1)$$
$$\times \left\{-3[\theta - \sin\theta - (\theta_i - \sin\theta_i)]\right.$$
$$\left. +2\left[\frac{(1 - \cos\theta)^2}{\sin\theta} - \frac{(1 - \cos\theta_i)^2}{\sin\theta_i}\right]\right\} . \qquad (4.8b)$$

$$g(\theta, \theta_i) = \frac{1}{2}b_m\left(\frac{\sin\theta}{1 - \cos\theta}\right)$$
$$\times \left\{\left(\frac{3}{2}b_m - 1\right)[\theta - \sin\theta - (\theta_i - \sin\theta_i)]\right.$$
$$\left. -(b_m - 1)\left[\frac{(1 - \cos\theta)^2}{\sin\theta} - \frac{(1 - \cos\theta_i)^2}{\sin\theta_i}\right]\right\} . \qquad (4.8c)$$

We see that the evolution of the radial scale factor a at given r_i depends on the initial conditions only through $\bar{\rho}_i$ and $(\partial b/\partial t)_i$ and their first derivatives with respect to r_i. The initial conditions are assumed to be chosen so that shell crossing does not occur, which requires $a \geq 0$ at all times. In the special case that the initial conditions have $\bar{\rho}_i$ and $(\partial b/\partial t)_i$ independent of r_i (i.e., a uniform density sphere in uniform expansion or contraction), $a(\theta) = b(\theta)$ at all later times, so that the collapse remains uniform. However, the generic case in which $\bar{\rho}_i$ and $(\partial b/\partial t)_i$ have nonvanishing gradients has very different behavior at late stages. A shell collapses to zero radius at $\theta = 2\pi$, corresponding to a time τ_c. Defining $\eta = 2\pi - \theta$, and expanding equations (4.6) and (4.8) for $\eta \ll 1$, one obtains

$$\begin{matrix} (\tau_c - \tau) \propto \eta^3 , & b \propto \eta^2 \propto (\tau_c - \tau)^{2/3} , \\ f \propto g \propto \eta^{-1} \propto (\tau_c - \tau)^{-1/3} , & a \propto \eta^{-1} \propto (\tau_c - \tau)^{-1/3} , \end{matrix} \qquad (4.9)$$

where in the last line, we assume that the coefficients of f and/or g are nonvanishing. Thus, in the generic case, $a \to \infty$ as $\tau \to \tau_c$, $b \to 0$, which is completely different from the special case of a uniform collapse, for which $a \to 0$ as $\tau \to \tau_c$, $b \to 0$. The ratio of the local density to the mean density within a shell evolves as $\rho/\bar{\rho} = b/a \propto (\tau_c - \tau)$ as $\tau \to \tau_c$, in the generic case, so that the mean interior density comes to dominate over the local density as the collapse proceeds, and the local dynamics approach those of a "vacuum" solution, in which all of the gravitating mass is concentrated at $r = 0$.

The above analysis can be applied to an arbitrary spherical collapse. We now specialize to the case of interest to galaxy formation, where the background flow consists initially of a small perturbation on top of a homogeneous, isotropic, expanding cosmological model. Thus, we express the density of the background flow as $\rho(r, t) = [1 + \delta(r, t)]\rho_b(t)$, and the mean density inside a sphere of radius r as $\bar{\rho}(r, t) = [1 + \bar{\delta}(r, t)]\rho_b(t)$, where $\rho_b(t)$ is the density of the homogeneous cosmological model, and δ and $\bar{\delta}$ are related by $\bar{\delta}(r) = (3/r^3)\int\delta(r')r'^2 dr'$. The perturbation grows until it reaches an amplitude $\bar{\delta} \simeq 1$, when it separate out from the expanding background and collapses. For spherical symmetry, the evolution of the perturbation can be calculated analytically into the

nonlinear regime by the method already described. Initial conditions are specified at a cosmic time t_i (measured from the big bang), assumed to be chosen such that $\bar{\delta}_i \ll 1$ and $|\Omega_i - 1| \ll 1$, where $\Omega \equiv 8\pi G \rho_b / 3H^2$ is the cosmological density parameter. Then at $t = t_i$, the cosmological background has density $\rho_{bi} \approx (1 + \delta_{ci})/6\pi G t_i^2$ and Hubble parameter $H_i \approx (1 - \frac{1}{3}\delta_{ci})(2/3t_i)$, where $\delta_{ci} \equiv \frac{3}{5}(\Omega_i - 1)$ (e.g., Peebles 1980, § 19). The background perturbation is assumed to consist of a pure growing density mode, so that $\bar{\rho}_i = [1 + \bar{\delta}_i(r_i)]\rho_{bi}$, $(\partial b/\partial t)|_i \approx [(1 - \frac{1}{3}\bar{\delta}_i(r_i)]H_i$ for $\bar{\delta}_i \ll 1$. (We consider only the growing density mode for the background density perturbation because even if a decaying density mode or a vorticity mode are present with comparable amplitudes at time t_i, they will become negligible compared to the growing mode for $t \gg t_i$.) Using equations (4.6), (4.5), and (4.3), the parametric solution for the evolution of the overdense region is given, to lowest order in $\bar{\delta}_i$, δ_{ci} as

$$b = \frac{r}{r_i} = \left[\frac{3}{10(\bar{\delta}_i + \delta_{ci})}\right](1 - \cos\theta), \qquad (4.10a)$$

$$\frac{t}{t_i} = \frac{3}{\sqrt{2}}\left[\frac{3}{10(\bar{\delta}_i + \delta_{ci})}\right]^{3/2}(\theta - \sin\theta). \qquad (4.10b)$$

Applying equation (4.1b) then gives

$$a = \left[\frac{3}{10(\bar{\delta}_i + \delta_{ci})}\right](1 - \cos\theta)$$

$$\times \left\{1 + \left[\frac{d\ln(\bar{\delta}_i + \delta_{ci})}{d\ln r_i}\right]\left[\frac{3}{2}\frac{\sin\theta(\theta - \sin\theta)}{(1 - \cos\theta)^2} - 1\right]\right\}. \quad (4.11)$$

Expressions (4.10) and (4.11) have fractional errors $O(\bar{\delta}_i)$, $O(\delta_{ci})$, which, however, can be made as small as desired by reducing t_i. We assume $(\bar{\delta}_i + \delta_{ci}) > 0$, and that $d\bar{\delta}_i/dr_i < 0$, so that the collapse time increases with initial radius. This solution is valid into the nonlinear regime up to shell crossing.

Henceforth, we assume that the background cosmology has $\Omega = 1$, so that $\delta_{ci} = 0$ (the results can easily be generalized to other values of Ω). A given spherical shell expands from radius $r = 0$ at $\theta = 0$, $t = 0$, reaches a maximum radius $r_m = (3/5\bar{\delta}_i)r_i$ at $\theta = \pi$, $t = t_m = (3\pi/4)(3/5\bar{\delta}_i)^{3/2}t_i$, and collapses back to $r = 0$ at $\theta = 2\pi$, $t = t_c = 2t_m$. For $\Omega = 1$, the background cosmology has density $\rho_b = 1/6\pi G t^2$, so that the mean overdensity within a shell evolves as

$$\bar{\delta}(\theta) \equiv \frac{\bar{\rho}(\theta)}{\rho_b(\theta)} - 1 = \frac{9}{2}\frac{(\theta - \sin\theta)^2}{(1 - \cos\theta)^3} - 1. \qquad (4.12)$$

In the linear regime $\theta \ll 1$, this reduces to

$$\bar{\delta} \approx \frac{3}{20}\theta^2 \approx \delta_i\left(\frac{\theta}{\theta_i}\right)^2 \approx \delta_i\left(\frac{t}{t_i}\right)^{2/3}, \qquad (4.13)$$

which is the usual result for a growing density mode in an $\Omega = 1$ cosmology.

b) Perturbation Equations

We now consider the growth of "subperturbations" on top of a spherical overdense region which is collapsing to form (say) a galaxy. Thus, the total density is expressed as $\rho(r, t) = \rho_b(t)[1 + \delta(r, t)][(1 + \epsilon(r, t)]$, with an analogous equation for the velocity. We assume that $\epsilon \ll 1$, and that the scale of the perturbation associated with ϵ is much smaller than that

associated with δ. When $\delta \ll 1$, the density can be expressed as $\rho \approx \rho_b(1 + \delta + \epsilon)$, and the ϵ and δ perturbations evolve independently according to the usual laws for the growth of linear perturbations in a cosmological model. However, for $\delta \gtrsim 1$, the evolution of δ significantly affects that of ϵ, because the small-scale ϵ perturbation sees a local background flow determined by δ.

The comoving and the proper wavevectors for the ϵ perturbation may be written as

$$\boldsymbol{q} = q(\cos\alpha, \sin\alpha, 0), \quad \boldsymbol{k} = q\left(\frac{\cos\alpha}{a}, \frac{\sin\alpha}{b}, 0\right), \quad (4.14)$$

where $\cos\alpha = \hat{\boldsymbol{q}} \cdot \hat{\boldsymbol{r}}$, and we have used the symmetry of the background flow around the radial direction to set one of the tangential components of $\boldsymbol{q}$ equal to zero. Defining $\cos\beta = \hat{\boldsymbol{k}} \cdot \hat{\boldsymbol{r}}$, the instantaneous orientation of the proper wavevector is given by $\tan\beta = (a/b)\tan\alpha$. For a generic spherical collapse, we have $d\bar{\delta}_i/dr_i < 0$ so that $\delta_i/\bar{\delta}_i < 1$, and thus $a/b \to \infty$ as $t \to t_c$. Therefore for generic initial conditions ($\alpha \neq 0, \pi/2$) the wavevector tends to become aligned with the tangential direction as the background collapse proceeds, and $\beta \to \pi/2$ as $t \to t_c$.

The peculiar momentum $\boldsymbol{V} \equiv (U, V, W)$ is related to the peculiar velocity $\boldsymbol{v} \equiv (u, v, w)$ by (eq. [2.33])

$$\boldsymbol{V} = (au, bv, bw). \qquad (4.15)$$

Then, by equation (2.27), $\boldsymbol{V}$ can be decomposed into mutually orthogonal pieces as

$$\boldsymbol{V} = V_{\parallel}\hat{\boldsymbol{q}} + \boldsymbol{V}_{\perp} + \boldsymbol{W}, \qquad (4.16a)$$

where

$$V_{\parallel} = U\cos\alpha + V\sin\alpha,$$

$$\boldsymbol{V}_{\perp} = V_{\perp}(\sin\alpha, -\cos\alpha, 0), \quad V_{\perp} = U\sin\alpha - V\cos\alpha,$$

$$\boldsymbol{W} = (0, 0, W). \qquad (4.16b)$$

The time evolution of the components of $\boldsymbol{V}$ perpendicular to $\boldsymbol{q}$ is $V_{\perp} = $ constant, $W = $ constant. The evolution of w is completely decoupled from that of ϵ, u, and v. With these definitions, and assuming an equation of state of the form $p \propto \rho^{\gamma}$, the evolution equations for perturbations (2.29) and (2.30) become

$$\frac{d\epsilon}{dt} = -i\left[\left(\frac{\cos^2\alpha}{a^2} + \frac{\sin^2\alpha}{b^2}\right)(qV_{\parallel})\right.$$

$$\left. - \sin\alpha\cos\alpha\left(\frac{1}{b^2} - \frac{1}{a^2}\right)(qV_{\perp})\right], \quad (4.17a)$$

$$\frac{d(qV_{\parallel})}{dt} = i\frac{4\pi G\rho_i\epsilon}{ab^2[(\cos^2\alpha)/a^2 + (\sin^2\alpha)/b^2]}$$

$$\times \left[1 - \frac{(q/q_{Ji})^2}{(ab^2)^{\gamma - 2}}\left(\frac{\cos^2\alpha}{a^2} + \frac{\sin^2\alpha}{b^2}\right)\right]. \quad (4.17b)$$

The second term in the brackets in equation (4.17b) is just $(k/k_J)^2 = (q/q_J)^2$, where $q_J(t)$ is the instantaneous comoving Jeans wavenumber. One sees that for $q \ll q_J(\lambda \gg \lambda_J)$, q, $V_{\parallel}$, and $V_{\perp}$ enter the evolution equations only through the combinations $qV_{\parallel}$ and $qV_{\perp}$.

In the form derived above, the perturbation equations depend implicitly on the time t_i at which initial conditions for the background perturbation are specified. This dependence

can be removed by defining a new set of variables:

$$a = \left(\frac{3}{10\bar{\delta}_i}\right)A(\theta) = \left(\frac{3}{10\bar{\delta}_i}\right)B(\theta)F(\theta) , \qquad (4.18a)$$

$$b = \left(\frac{3}{10\bar{\delta}_i}\right)B(\theta) , \qquad (4.18b)$$

$$t = \frac{3}{4}\left(\frac{3}{5\bar{\delta}_i}\right)^{3/2} t_i T(\theta) , \qquad (4.18c)$$

where

$$B(\theta) \equiv (1 - \cos\theta) , \qquad (4.18d)$$

$$F(\theta) \equiv 1 + 3\Delta\left[1 - \frac{3}{2}\frac{\sin\theta(\theta - \sin\theta)}{(1 - \cos\theta)^2}\right] , \qquad (4.18e)$$

$$T(\theta) \equiv (\theta - \sin\theta) , \qquad (4.18f)$$

$$\Delta \equiv 1 - \frac{\delta_i}{\bar{\delta}_i} ; \qquad (4.18g)$$

$F(\theta)$ is a direct measure of the anisotropy of the scale factors. With these variables, $\tan\beta = F(\theta)\tan\alpha$. We also define dimensionless velocity variables and wavevectors:

$$(\tilde{U}, \tilde{W}, \tilde{W}) \equiv -i(15\bar{\delta}_i)^{1/2}qt_i(U, V, W) , \qquad (4.19a)$$

$$(\tilde{u}, \tilde{v}, \tilde{w}) \equiv \left(\frac{\tilde{U}}{A}, \frac{\tilde{V}}{B}, \frac{\tilde{W}}{B}\right) , \qquad (4.19b)$$

$$\tilde{q} \equiv qr_i , \qquad (4.19c)$$

$$Q^2 \equiv \left(\frac{10\bar{\delta}_i}{3}\right)^{3\gamma-4}\left(\frac{q}{q_{Ji}}\right)^2 . \qquad (4.19d)$$

For a given physical perturbation on a given background solution, the values of $\tilde{U}$, $\tilde{V}$, $\tilde{W}$, $\tilde{q}$, and Q are independent of t_i, assuming that t_i has been chosen such that $\bar{\delta}_i \ll 1$. The quantities $\delta_i/\bar{\delta}_i$ and α are also independent of t_i under the same conditions. The peculiar velocity in physical units can be derived from the relation

$$(u, v, w) = \left[\frac{2}{3}\left(\frac{5\bar{\delta}_i}{3}\right)^{1/2}\frac{r_i}{t_i}\right]\frac{i}{\tilde{q}}(\tilde{u}, \tilde{v}, \tilde{w})$$

$$= \left(\frac{\pi r_m}{2t_m}\right)\frac{i}{\tilde{q}}(\tilde{u}, \tilde{v}, \tilde{w}) . \qquad (4.20)$$

Since $A \simeq B \simeq 1$ at turnaround, $Q \simeq q/q_{Jm}$, where q_{Jm} is the comoving Jeans wavenumber at turnaround. The short-wavelength assumption requires that $\tilde{q} \ll 1$, while the assumption that pressure has a negligible effect on on the background flow requires $\tilde{q}_J \gg 1$.

In terms of the dimensionless variables defined above the evolution equations for perturbations (4.17a) and (4.17b) become

$$\frac{d\epsilon}{d\theta} = \frac{1}{F^2B}\left[(\cos^2\alpha + F^2\sin^2\alpha)\tilde{V}_\parallel\right.$$
$$\left. - \sin\alpha\cos\alpha(F^2 - 1)\tilde{V}_\perp\right] , \qquad (4.21a)$$

$$\frac{d\tilde{V}_\parallel}{d\theta} = \frac{3F\epsilon}{(\cos^2\alpha + F^2\sin^2\alpha)}$$
$$\times\left[1 - \frac{Q^2}{F^\gamma B^{3\gamma-4}}(\cos^2\alpha + F^2\sin^2\alpha)\right] . \qquad (4.21b)$$

Solution of these equations gives four independent modes. One mode has $\tilde{w} = \tilde{W}/B$ and $\epsilon = \tilde{u} = \tilde{v} = 0$. Since the evolution of this mode is trivial, it will not be further discussed. Below we consider the evolution of the remaining modes having $\tilde{W} = 0$ and $\epsilon, \tilde{U}, \tilde{V} \neq 0$.

c) Evolution of Perturbations with Zero Pressure: Asymptotic Analyses

We consider first the evolution of perturbations for which pressure is completely negligible; i.e., we assume that $\lambda \gg \lambda_J$ at all stages of the collapse. This corresponds to setting $Q = 0$ in equations (4.21a), (4.21b). Since we are assuming $\tilde{W} = 0$, there are three independent modes, two of which may be taken to have zero vorticity ($\tilde{V}_\perp = 0$). The evolution of these modes in the generic case $\delta_i/\bar{\delta}_i < 1$, $\alpha \neq 0$, $\pi/2$ is qualitatively as follows: In the limit $\theta \to 0$ ($t \to 0$), the anisotropy factor $F \to 1$, and the expansion is isotropic: $a = b \propto \theta^2 \propto t^{2/3}$. The vorticity-free modes asymptotically have the same behavior as in an $\Omega = 1$ cosmology (e.g., Weinberg 1972, § 15.9): there are a growing and a decaying density mode. The vorticity mode becomes purely transverse in this limit. The evolution of zero-vorticity perturbations in this regime is independent of the orientation of the wavevector, which remains constant, $\beta = \alpha$. At $\theta = \pi$, the radial expansion of a spherical shell turns around, as does the local expansion in the tangential direction. In general, the initially decaying density mode begins to grow again at around this time. The anisotropy factor F grows monotonically, and becomes significantly greater than 1 for $\theta > \theta_F(\Delta) \gtrsim 1$, where θ_F increases with decreasing Δ. More precisely, if we define θ_F by $F(\theta_F) = 2$, then $\theta_F \approx 2.2$ for $\Delta = 1$, and $\theta_F \approx 2\pi - (36\pi\Delta)^{1/3}$ for $\Delta \ll 1$ (recall that $\Delta > 0$). Once the local expansion becomes anisotropic, with $a > b$, the wavevector of the perturbation begins to be sheared around toward the tangential direction. Furthermore, the density perturbation associated with the vorticity mode becomes significant. For $\theta \to 2\pi$ ($t \to t_c$), $F \to \infty$, and any perturbation with $\alpha \neq 0$ is sheared around to have its wavevector tangential, $\beta = \pi/2$. In this limit, $\epsilon \to \infty$ and $\tilde{u}/\tilde{v} \to 0$ in the generic case, and the evolution of $(\epsilon, \tilde{v})$ for a vorticity mode becomes indistinguishable from that for a vorticity-free mode [although the ratio $\tilde{V}_\perp/\tilde{V}_\parallel$ remains different for the two types, and thus $\tilde{u}$ is different for given $(\epsilon, \tilde{v})$]. With the exception of certain special (and atypical) cases discussed below, the full evolution of the perturbations over the range $0 \leq \theta \leq 2\pi$ can be determined only by integrating the equations numerically. However, the asymptotic behavior in the limits $\theta \to 0$ and $\theta \to 2\pi$ may be calculated analytically, as we now discuss.

i) Behavior for $\theta \to 0$

In this limit we have, expanding equations (4.18d)–(4.18f) in powers of θ:

$$t \propto T \sim \theta^3/6 , \qquad (4.22a)$$

$$B \sim \theta^2/2 \propto t^{2/3} , \qquad (4.22b)$$

$$F \sim 1 + \tfrac{3}{20}\Delta\theta^2 , \qquad (4.22c)$$

The behavior of perturbations may be found by combining equations (4.21a) and (4.21b) into a single second-order differential equation for ϵ analogous to equation (2.34), expanding the coefficients in this equation in powers of θ, and then looking for power series solutions. For the zero-vorticity

modes ($\tilde{V}_\perp = 0$), one finds a growing solution

$$\epsilon \sim \frac{3}{20}\left(\frac{\epsilon_{i1}}{\bar{\delta}_i}\right)\theta^2 , \qquad \tilde{V}_\parallel \sim \frac{3}{20}\left(\frac{\epsilon_{i1}}{\bar{\delta}_i}\right)\theta^3 ,$$

$$\tilde{u} \sim \frac{3}{10}\left(\frac{\epsilon_{i1}}{\bar{\delta}_i}\right)\theta\cos\alpha , \qquad \tilde{v} \sim \frac{3}{10}\left(\frac{\epsilon_{i1}}{\bar{\delta}_i}\right)\theta\sin\alpha ,$$

(4.23)

and a decaying solution

$$\epsilon \sim \left(\frac{20}{3}\right)^{3/2}(\epsilon_{i2}\bar{\delta}_i^{3/2})\frac{1}{\theta^3} ,$$

$$\tilde{V}_\parallel \sim -\frac{3}{2}\left(\frac{20}{3}\right)^{3/2}(\epsilon_{i2}\bar{\delta}_i^{3/2})\frac{1}{\theta^2} ,$$

$$\tilde{u} \sim -3\left(\frac{20}{3}\right)^{3/2}(\epsilon_{i2}\bar{\delta}_i^{3/2})\frac{1}{\theta^4}\cos\alpha ,$$

$$\tilde{v} \sim -3\left(\frac{20}{3}\right)^{3/2}(\epsilon_{i2}\bar{\delta}_i^{3/2})\frac{1}{\theta^4}\sin\alpha ,$$

(4.24)

where ϵ_{i1} and ϵ_{i2} are the amplitudes of these modes at the time θ_i, when the background perturbation has amplitude $\bar{\delta}_i \approx (3/20)\theta_i^2$. The vorticity mode can be taken to have the dependence

$$\epsilon \sim \frac{3}{10}\Delta\sin\alpha\cos\alpha\,\tilde{V}_\perp\theta , \quad \tilde{V}_\parallel \sim \frac{9}{20}\Delta\sin\alpha\cos\alpha\,\tilde{V}_\perp\theta^2 ,$$

$$\tilde{u} \sim \frac{2\tilde{V}_\perp}{\theta^2}\sin\alpha, \qquad\qquad \tilde{v} \sim -\frac{2\tilde{V}_\perp}{\theta^2}\cos\alpha ,$$

(4.25)

We note that for $\Delta = 0$ or $\alpha = 0$ or $\alpha = \pi/2$, we have $\epsilon = \tilde{V}_\parallel = 0$ for this mode.

We define "growing density," "decaying density," and "vorticity" modes as being those solutions of the exact linearized perturbation equations having the asymptotic behaviors given by equations (4.23), (4.24), and (4.25), respectively. The asymptotic behavior of the zero vorticity modes is the same as one obtains from the analysis of § III for a mode with wavevector along a principal axis. For $t \to 0$, we have $a \sim b \propto t^{2/3}$, corresponding to case ($a[\text{ii}]$) (with $\alpha_1 = \frac{2}{3}$, $\beta = 2$), so that self-gravity and kinematics are of comparable importance.

ii) Behavior for $\theta \to 2\pi\,(\delta_i/\bar{\delta}_i < 1, \alpha \neq 0)$

We expand equations (4.18d)–(4.18f) in powers of $\eta \equiv 2\pi - \theta$, obtaining

$$(t_c - t) \propto (2\pi - T) \sim \eta^3/6 , \tag{4.26a}$$

$$B \sim \eta^2/2 \propto (t_c - t)^{2/3} , \tag{4.26b}$$

$$F \sim 36\pi\Delta/\eta^3 \propto (t_c - t)^{-1} , \tag{4.26c}$$

This scaling of the expansion factors with time applies to the endpoint of spherical collapse from any generic initial conditions (see eqs. [4.9]), so the results derived below are valid for any such collapse. One can again find three independent power series solutions. These, however, do *not* correspond in a one-to-one way with the three solutions for $\theta \to 0$ listed above. Of the two zero-vorticity solutions, one is a density perturbation which grows as $\eta \to 0$:

$$\epsilon \sim \frac{c_1}{\eta} , \qquad\qquad \tilde{V}_\parallel \sim \frac{1}{2}c_1\csc^2\alpha ,$$

$$\tilde{u} \sim c_1\frac{\csc\alpha\cot\alpha}{36\pi\Delta}\eta , \quad \tilde{v} \sim c_1\csc\alpha\frac{1}{\eta^2} ,$$

(4.27)

and the other is a density perturbation which is neutral as $\eta \to 0$:

$$\epsilon \sim c_2 , \qquad\qquad \tilde{V}_\parallel \sim -c_2\frac{\csc^2\alpha}{48\pi\Delta}\eta^4 ,$$

$$\tilde{u} \sim -c_2\frac{\csc\alpha\cot\alpha}{6(12\pi\Delta)^2}\eta^5 , \quad \tilde{v} \sim -c_2\frac{\csc\alpha}{24\pi\Delta}\eta^2 .$$

(4.28)

There is a third independent solution having nonzero vorticity:

$$\epsilon \sim -\frac{\cot\alpha\,\tilde{V}_\perp}{10(18\pi\Delta)^2}\eta^5 , \quad \tilde{V}_\parallel \sim \cot\alpha\,\tilde{V}_\perp ,$$

$$\tilde{u} \sim \frac{\csc\alpha\,\tilde{V}_\perp}{18\pi\Delta}\eta , \qquad \tilde{v} \sim \frac{\csc\alpha\cot\alpha\,\tilde{V}_\perp}{30(18\pi\Delta)^3}\eta^7 .$$

(4.29)

The behavior of the zero-vorticity solutions in this limit is the same as one derives from the analysis of § III for a purely tangential perturbation ($\beta = \pi/2$), with $a \propto (t_c - t)^{-1/3}$, $b \propto (t_c - t)^{2/3}$. We have case ($a[\text{i}]$) ($\alpha_1 = \frac{2}{3}$, $\beta = 1$), in which density evolution is determined by the background kinematics, the self-gravity of the perturbation being negligible. The background flow corresponds to contraction along the direction of the wavevector, resulting in the existence of a solution with growing density.

The modes defined by the $\theta \to 0$ behavior specified in § IVc(i) can in the limit $\eta \to 0$ each be represented as linear combinations of the asymptotic solutions (4.27), (4.28), and (4.29). The two zero-vorticity modes map to linear combinations of the two zero-vorticity asymptotic solutions, while the vorticity mode maps to a linear combination of all three asymptotic solutions. As $\eta \to 0$, the c_1 solution dominates in ϵ and $\tilde{v}$, so that all three modes defined in § IVc(i) generically have the same (ϵ, $\tilde{v}$) behavior, up to scale factors. The reason why zero-vorticity and vorticity modes show this convergence in behavior is that any initial velocity component gets sheared around to being tangential, and density growth in this limit results entirely from the kinematic effect of the tangential velocity. The (linear) relations between c_1, c_2, and ϵ_{i1}, ϵ_{i2}, $\tilde{V}_\perp$ can be determined only by integrating the full equations over the range $0 \leq \theta \leq 2\pi$. However, this analysis does demonstrate that for generic initial conditions at $t \to 0$, one ends up with a growing density perturbation as $t \to t_c$, with $\epsilon \propto (t_c - t)^{-1/3}$ and the wavevector tangential.

iii) Behavior for $\theta \to 2\pi\,(\delta_i/\bar{\delta}_i < 1, \alpha = 0)$

For the special case that the wavevector is initially exactly radial, it remains radial at all later times ($\beta = 0$), so that the perturbed solution is a function only of (r, t). Therefore vorticity perturbations completely decouple from density perturbations. Ryden and Gunn (1987) have derived an exact analytic solution for this case (eq. [28] of their paper), corresponding to growing mode initial conditions (eq. [4.23]). Here we derive the asymptotic behaviors of the solutions as $\theta \to 2\pi$ by expanding in powers of η. Of the zero-vorticity solutions, one has neutral density behavior as $\eta \to 0$:

$$\epsilon \sim c_1 , \qquad \tilde{V}_\parallel \sim (54\pi\Delta)c_1/\eta^2 ,$$
$$\tilde{u} \sim 3c_1/\eta , \quad \tilde{v} = 0 ,$$

(4.30)

while the other has decaying density as $\eta \to 0$;

$$\epsilon \sim c_2\eta^5 , \qquad \tilde{V}_\parallel \sim -10(18\pi\Delta)^2 c_2 ,$$
$$\tilde{u} \sim -10(18\pi\Delta)c_2\eta , \quad \tilde{v} = 0 .$$

(4.31)

The zero-vorticity modes map to linear combinations of solutions (4.30) and (4.31). The vorticity mode has asymptotic behavior:

$$\epsilon = 0 , \qquad \widetilde{V}_\parallel = 0 ,$$
$$\tilde{u} = 0 , \qquad \tilde{v} \sim 2\widetilde{V}_\perp/\eta^2 . \tag{4.32}$$

The behavior of the zero-vorticity modes is the same as one derives from the analysis of § III, case $(a[\text{ii}])$ $(\alpha_1 = -\frac{1}{3}, \beta = 1)$, so that again the kinematic effect dominates over self-gravity. In this case, however, the background kinematics correspond to expansion along the direction of the wavevector, which causes the growth of any density perturbation to freeze out to a constant value as $t \to t_c$, which is completely different from the behavior in the generic case $\alpha \neq 0$. Thus, contrary to the assumption made by Ryden and Gunn, the results for radial perturbations are not representative of the general case.

For the other special case that the wavevector is initially exactly tangential $(\alpha = \pi/2)$, we have $\beta = \pi/2$, and again there is decoupling of vorticity and density perturbations. In this case, however, the limiting behavior for $\theta \to 2\pi$ is given correctly by setting $\alpha = \pi/2$ in the expressions derived in § IVc(ii) for the generic case.

iv) Behavior for $\theta \to 2\pi (\delta_i/\bar{\delta}_i = 1)$

If $\delta_i/\bar{\delta}_i = 1$ exactly $(\Delta = 0)$, then $F = 1 (a = b)$ at all times. This background solution corresponds to collapse of a uniform density sphere, which remains uniform at all times. The behavior of perturbations is exactly the same as for a cosmological model with $\Omega > 1$. Exact solutions for this case are given by Weinberg (1972, § 15.9), for instance. Since the expansion is isotropic, vorticity perturbations are decoupled from density perturbations, and the evolution is independent of the orientation angle α. The limiting behavior of the solutions is as follows: of the zero-vorticity solutions, one has growing density as $\eta \to 0$:

$$\epsilon \sim c_1/\eta^3 , \qquad \widetilde{V}_\parallel \sim (\tfrac{3}{2})c_1/\eta^2 ,$$
$$\tilde{u} \sim 3c_1/\eta^4 \cos \alpha , \qquad \tilde{v} \sim 3c_1/\eta^4 \sin \alpha , \tag{4.33}$$

and the other has decaying density as $\eta \to 0$:

$$\epsilon \sim c_2 \eta^2 , \qquad \widetilde{V}_\parallel \sim -c_2 \eta^3 ,$$
$$\tilde{u} \sim -2c_2 \eta \cos \alpha , \qquad \tilde{v} \sim -2c_2 \eta \sin \alpha . \tag{4.34}$$

The vorticity mode has the dependence

$$\epsilon = 0 , \qquad \widetilde{V}_\parallel = 0 ,$$
$$\tilde{u} \sim \frac{2\widetilde{V}_\perp}{\eta^2} \sin \alpha , \qquad \tilde{v} \sim -\frac{2\widetilde{V}_\perp}{\eta^2} \cos \alpha . \tag{4.35}$$

The limiting behavior of the scale factors is $a = b \propto (t_c - t)^{2/3}$, so the evolution of the density perturbations can be obtained from the analysis of § III, case $(a[\text{iii}])$ $(\alpha_1 = \tfrac{2}{3}, \beta = 2)$, so that self-gravity and the kinematics make comparable contributions to the growth of density perturbations, in contrast to the case $\delta_i/\bar{\delta}_i < 1$, where the behavior at late stages is given entirely by the kinematic effect. As a result, the growth of density perturbations as $t \to t_c$ is much faster in the special case $\delta_i/\bar{\delta}_i = 1$, which has $\epsilon \propto (t_c - t)^{-1}$ for the growing mode, than in the generic case $\delta_i/\bar{\delta}_i < 1$, which has $\epsilon \propto (t_c - t)^{-1/3}$.

d) Evolution of Perturbations with Zero Pressure: Numerical Integrations

The complete behavior of the perturbations for zero pressure is found by numerical integration of equations (4.21a) and (4.21b) with $Q = 0$. The initial conditions can be specified in terms of the amplitudes $\epsilon_{i1}/\bar{\delta}_i$, $\epsilon_{i2} \bar{\delta}_i^{3/2}$ and $\widetilde{V}_\perp$ of the three modes having the dependences given by equations (4.23), (4.24), and (4.25) as $\theta \to 0$. If whatever mechanism generates the initial perturbations operates at a time long before the background perturbation goes nonlinear, as is generally assumed to be the case for galaxy formation, then only the perturbations developing from growing-mode initial conditions are likely to be important for formation of substructure during the collapse of a protogalaxy. For suppose that at $\theta_i \ll 1$ all three modes are generated with equal values of the peculiar velocity $(\tilde{u}^2 + \tilde{v}^2)^{1/2}$. Then at some later $\theta \ll 1$, the density amplitudes of the three modes are in the ratio (growing:decaying:vorticity) $= 1 : (\tfrac{2}{3})(\theta_i/\theta)^5 : (3/10)\Delta \sin \alpha \cos \alpha \theta_i^3/\theta$. Therefore for $\sin \alpha \simeq \cos \alpha \simeq 1$, when the background perturbation becomes nonlinear at $\theta \simeq 1$, the density amplitudes of the decaying and vorticity modes are suppressed relative to that of the growing mode by factors of the order θ_i^5 and $\Delta\theta_i^3$, respectively. Numerical integrations show that these bounds on the relative density amplitudes remain correct to order of magnitude during the nonlinear collapse of the background perturbation. Therefore, only results for growing mode initial conditions will be presented here. In this case, the amplitude of the perturbation scales linearly with $\epsilon_i/\bar{\delta}_i$, so that the only parameters which need to be specified in a numerical calculation are $\Delta = (1 - \delta_i/\bar{\delta}_i)$ and α.

Figure 1 shows the evolution of the scale factors A and B as a function of θ for $\delta_i/\bar{\delta}_i = (1, 0.9, 0.7, 0, -2)[\Delta = (0, 0.1, 0.3, 1, 3)]$, and Figures 2–6 show the evolution of the density amplitude ϵ and the peculiar velocity components $\tilde{u}, \tilde{v}$ for the same values of $\delta_i/\bar{\delta}_i$ and for $\alpha = (0°, 10°, 30°, 90°)$, the curves being normalized to $\epsilon_i/\bar{\delta}_i = 1$. The figures also show the $\theta \to 0$ asymptote to $\epsilon(\theta)$ given by equation (4.23), which is the same as the perturbation behavior in a homogeneous $\Omega = 1$ background. Values $\delta_i/\bar{\delta}_i < 0$ represent an underdense region $(\delta_i < 0)$ surrounding an overdense region $(\bar{\delta}_i > 0)$. For comparison purposes, it is convenient to take the behavior for $\delta_i/\bar{\delta}_i = 1 (\Delta = 0)$ as a standard case. For $\delta_i/\bar{\delta}_i = 1$, perturbation growth is independent of α. For $\delta_i/\bar{\delta}_i < 1$, perturbation growth follows that for $\delta_i/\bar{\delta}_i = 1$ at small θ, and then falls below when
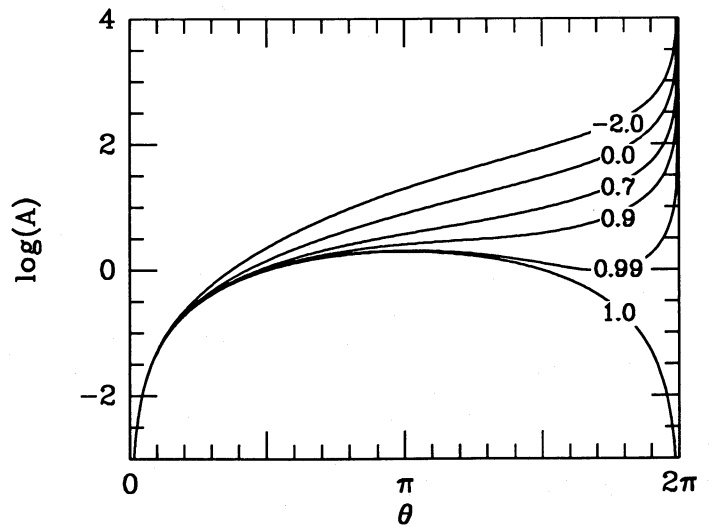

FIG. 1.—Evolution of local scale factors for spherical background flow. Curves show radial scale factor $A(\theta)$ and are labeled with value of $\delta_i/\bar{\delta}_i$. Tangential scale factor $B(\theta)$ is same for all $\delta_i/\bar{\delta}_i$, and equal to $A(\theta)$ for $\delta_i/\bar{\delta}_i = 1$.
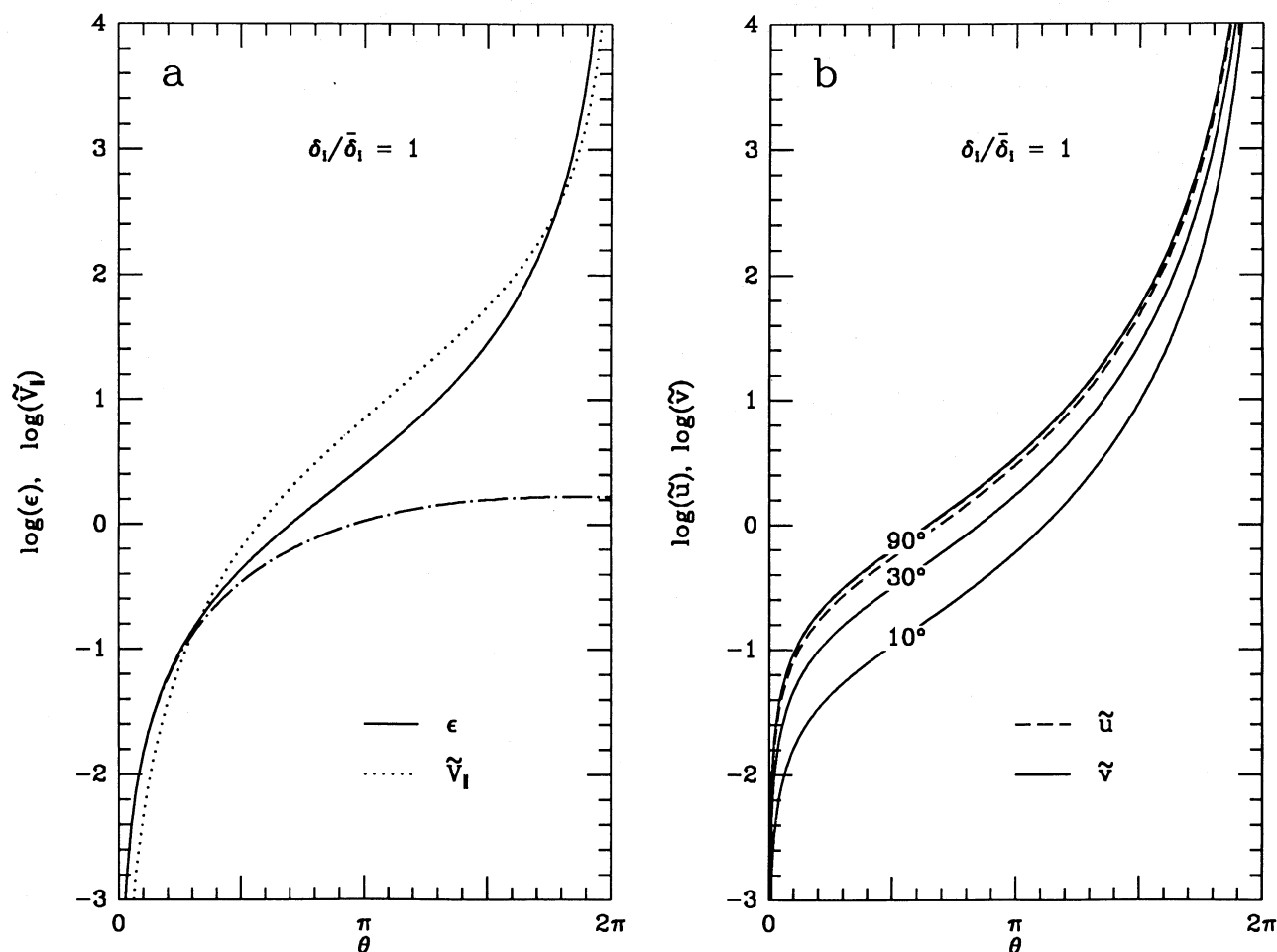
FIG. 2.—Evolution of perturbations in spherical background flow for $\delta_i/\bar{\delta}_i = 1$ and inclination angle $\alpha = (0°, 10°, 30°, 90°)$. (a) Density perturbation ϵ and longitudinal peculiar momentum $\tilde{V}_\parallel$. Curves are idential for all values of α. Also shown is the evolution of ϵ in an $\Omega = 1$ cosmology (dash-dotted curve). (b) Radial peculiar velocity $\tilde{u}$ and tangential peculiar velocity $\tilde{v}$. Curves are labeled by value of α. (Labeling on $\tilde{u}$ curves suppressed for clarity; it runs in the opposite sense vertically to that on $\tilde{v}$ curves).

$F \gtrsim 2$. Two factors cause the perturbation amplitude at a given value of θ to be suppressed relative to the standard case (see eq. [2.34]): (i) the local background density is smaller than in the standard case (since $\rho \propto 1/ab^2$), so the self-gravity of the perturbation is smaller; (ii) the scale factor along the direction of the wavevector is larger than in the standard case for any perturbation which is not tangential, so growth due to the kinematic effect is smaller. For exactly tangential perturbations ($\alpha = \pi/2$), only effect (i) operates, while the kinematics still favor growth, so that as $\theta \to 2\pi$ (when kinematic effects dominate over self-gravity), the perturbation amplitude ϵ diverges (but less rapidly than for $\delta_i/\bar{\delta}_i = 1$). For exactly radial perturbations ($\alpha = 0$), both suppression effects operate, so that the amplitude for such perturbations is less than in the tangential case, and at late stages the growth of ϵ is halted completely. Intermediate values of α give intermediate behavior. For $\alpha \lesssim 1$, perturbation growth at first approximates that for $\alpha = 0$, until the wavevector is sheared around to being nearly tangential, which occurs for $F \tan \alpha \simeq 1$, after which the growth tracks that for $\alpha = \pi/2$.

e) Evolution of Perturbations with Pressure

We now consider the effects on perturbation evolution of including the pressure. To simplify the discussion, assume zero

perturbed vorticity. The background evolution is assumed to follow the pressure-free solution as before; a rough criterion for pressure forces to be negligible compared to gravity for the background solution is $c_s^2/4\pi G\bar{\rho}r^2 \ll 1$. The pressure is assumed to vary as $p \propto \rho^\gamma$. In practice, we are most interested in values in the range $1 \leq \gamma \leq 5/3$. For the case of galaxy formation, the thermal evolution of the gas at early times is actually more complicated than this simple polytropic behavior because of the interaction of the matter with the radiation. We do not attempt to treat this in detail, but instead simply assume that evolution at constant γ is valid at least for the later stages ($\theta \gtrsim \pi$, say). The effects of pressure are then entirely parametrized in terms of Q. We recall that $Q \simeq \lambda_J/\lambda$ at turnaround ($\theta = \pi$), so that a perturbation with $Q \gtrsim 1$ will oscillate at this time, while one with $Q \lesssim 1$ will tend to grow. The detailed behavior can only be found by numerical integration, but as $\theta \to 2\pi$ it must match onto the asymptotic dependence which we now derive.

The evolution of density perturbations in the limit $t \to t_c(\theta \to 2\pi)$ can be determined analytically using the analysis of § III. (i) for the generic case ($\delta_i/\bar{\delta}_i < 1$, $\alpha \neq 0$), any perturbation becomes tangential in this limit, so we have $\alpha_1 = \frac{2}{3}$, $\beta = 1$ in the notation of that section. For $2/3 < \gamma < 5/3$ (case IIIb[i]), pressure dominates self-gravity in this limit, but the
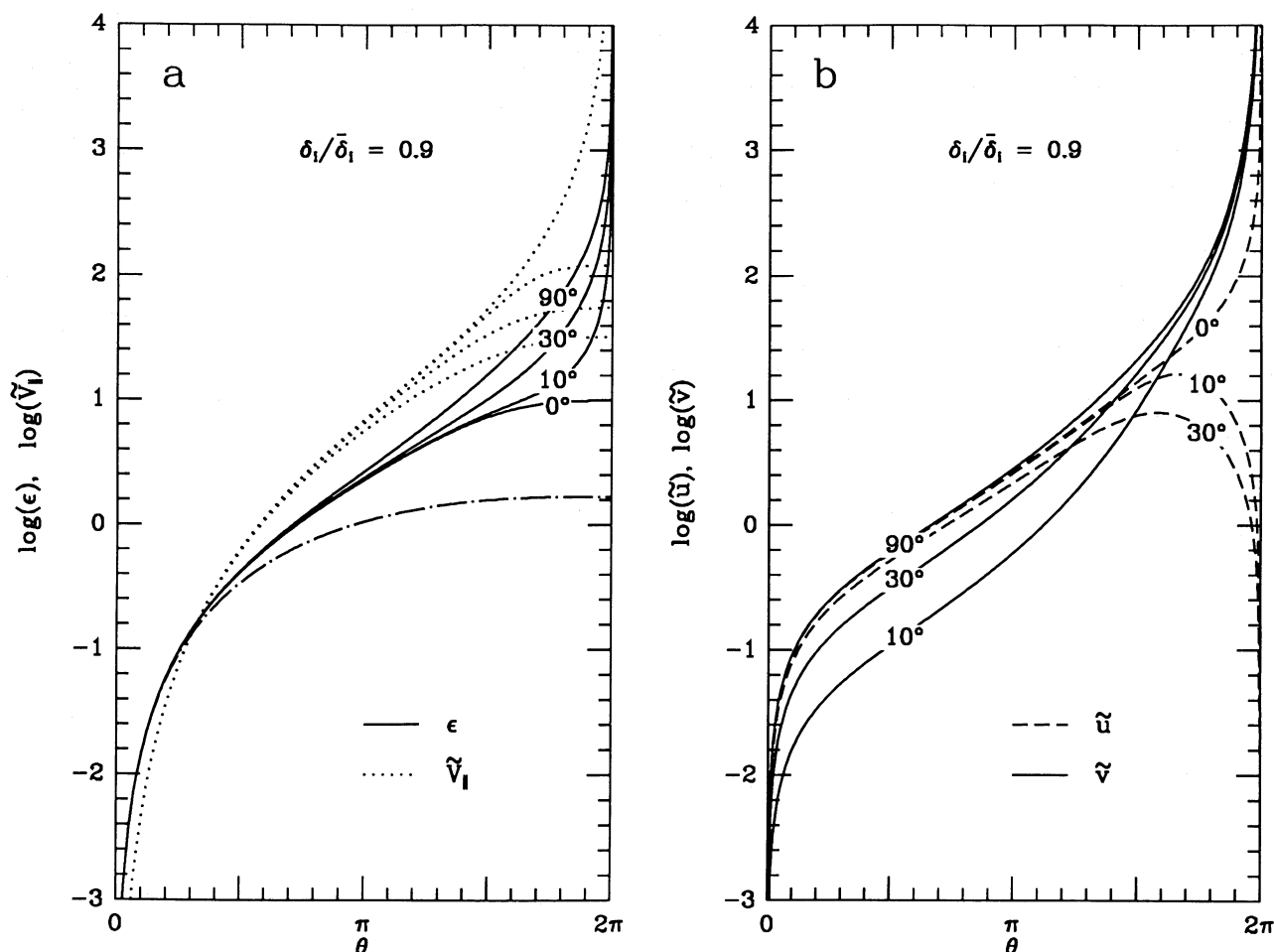
Fig. 3.—Evolution of perturbations in spherical background flow for $\delta_i/\bar{\delta}_i = 0.9$. Coding to curves is same as in Fig. 2. (Labeling of $\tilde{V}_\parallel$ curves by value of α suppressed for clarity; it runs in the opposite sense vertically to that on ϵ curves).

kinematic effect dominates both, so the asymptotic behavior is the same as for $p = 0$, with the density growing as $\epsilon \propto (t_c - t)^{-1/3}$. For $\gamma > 5/3$ (case IIIb[iii]), the effects of pressure dominate over kinematics and self-gravity, and the perturbation density ϵ rapidly oscillates, with oscillation amplitude varying as $(t_c - t)^{-(7-3\gamma)/12}$. For the special case $\gamma = 5/3$ (case IIIb[ii]), a more detailed analysis based on equations (4.21a) and (4.21b) shows that ϵ has power-law behavior in $t_c - t$ in this limit, with the exponents being real or complex, depending on whether $Q < Q_c$ or $Q > Q_c$, respectively, where $Q_c = [(\sqrt{3\pi\Delta})/16]^{1/3}$. In either case, ϵ grows more slowly than for $\gamma < 5/3$. (ii) For the special case of radial perturbations ($\delta_i/\bar{\delta}_i < 1$, $\alpha \neq 0$), we have $\alpha_1 = -1/3$, $\beta = 1$. Provided $\gamma < 8/3$, pressure becomes negligible compared to self-gravity in this limit (case IIIa[i]), and the behavior is the same as for $p = 0$, with $\epsilon \to$ constant. (iii) For the special case of a uniform collapse ($\delta_i/\bar{\delta}_i = 1$, α arbitrary), we have $\alpha_1 = 2/3$, $\beta = 2$. Thus for $\gamma < 4/3$ (case IIIa[ii]), pressure becomes negligible in this limit, so the asymptotic behavior is the same as for $p = 0$, with $\epsilon \propto (t_c - t)^{-1}$. For $\gamma > 4/3$ (case IIIb[iii]), pressure dominates self-gravity and kinematics, and ϵ rapidly oscillates, with oscillation amplitude varying as $(t_c - t)^{-(5-3\gamma)/6}$.

V. PLANAR BACKGROUND FLOW

a) Background Flow

Another case for which one can derive an exact solution for the evolution of a cosmological perturbation into the nonlinear regime is that in which the perturbation has planar symmetry, with zero pressure and no crossing of planes of matter (e.g., Zel'dovich and Novikov 1983, § 14.2). The analogous problem for a finite system is the collapse of a homogeneous spheroid, for which the solution is found by integrating a set of ordinary differential equations (e.g., Peebles 1980, § 20). In either case, the final stages of the collapse are characterized by a "pancake" singularity, in which particle separations shrink to zero along the direction perpendicular to the plane of the pancake, but remain finite along the two perpendicular ("tangential") directions. We consider only the cosmological case in detail.

We first derive the form of the background flow. Take the symmetry plane to be $x = 0$, so that collapse occurs parallel to the x-direction. The principal axes of the flow are along the collapse (x) direction and along any two orthogonal tangential
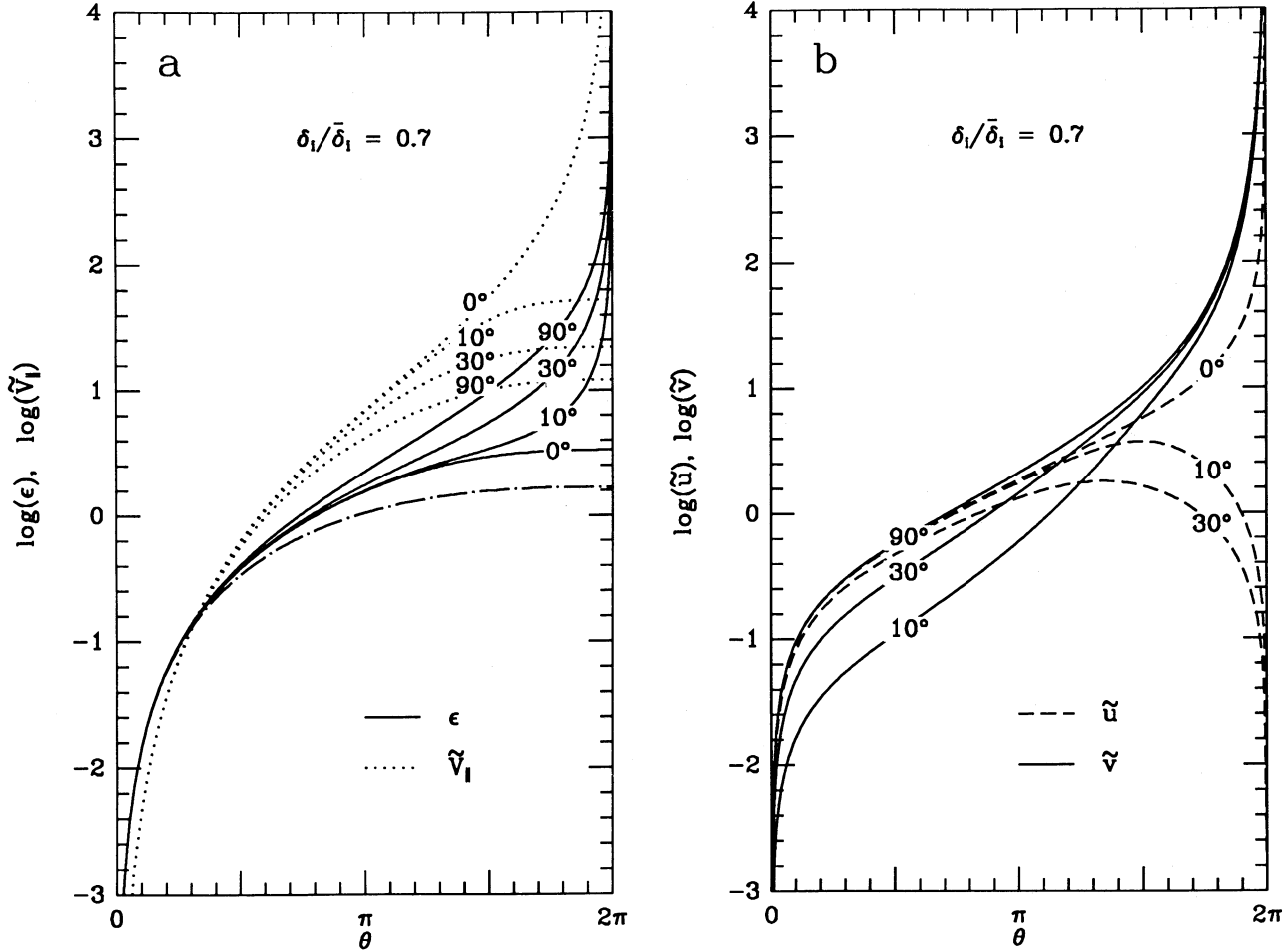
FIG. 4.—Evolution of perturbations in spherical background flow for $\delta_i/\bar{\delta}_i = 0.7$. Coding curves is same as in Fig. 2.

(y, z) directions. Then $A_{ij}(t) = \text{diag}(a, b, b)$, where

$$a = \left.\frac{\partial x}{\partial x_i}\right|_t , \tag{5.1a}$$

$$b = \left.\frac{\partial y}{\partial y_i}\right|_t = \left.\frac{\partial z}{\partial z_i}\right|_t . \tag{5.1b}$$

The exact equations of motion of a fluid particle, including the background perturbation, are

$$\frac{D^2 r}{Dt^2} = -\frac{4\pi}{3} G\rho_b(t)r - 4\pi G\,\delta\sigma(x, t)\hat{x} , \tag{5.2}$$

where

$$\delta\sigma(x, t) \equiv \int_0^x [\rho(x', t) - \rho_b(t)]dx'$$

is the perturbation in the surface density within distance x of the symmetry plane. For the transverse (y, z) directions equation (5.2) reduces to the unperturbed Friedmann equation, so that $b(t)$ is the same as the scale factor for the background cosmological model, and $\rho_b(t) = \rho_{bi}/b^3(t)$. The remaining component of equation (5.2) can be solved by defining the Lagrangian coordinate $s \equiv \sigma/\rho_b(t)b(t)$, where

$$\sigma(x, t) = \int_0^x \rho(x', t)dx'$$

is the exact surface density, and writing $x(s, t) = b(t)s + \delta x(s, t)$.

This gives

$$\left.\frac{\partial^2 \delta x}{\partial t^2}\right|_s = \frac{8\pi}{3} G\rho_b(t)\delta x . \tag{5.3}$$

This equation has a growing solution and a decaying solution. Write the growing solution as $D(t)$, with normalization $D(t_i) = 1$; assuming that only this solution is present, we have

$$x(s, t) = b(t)s + D(t)\psi(s) , \tag{5.4}$$

where $\psi(-s) = -\psi(s)$. The function $\psi(s)$ may be related to the initial density perturbation $\delta_i(s)$ by noting that $\rho_i/\rho_{bi} = (\partial s/\partial x_i)$. This gives, for $\delta_i \ll 1$,

$$d\psi/ds \approx -\delta_i(s) ,$$

and

$$\psi(s) \approx -\int_0^s \delta_i(s')ds' \equiv -s\bar{\delta}_i(s) .$$

Therefore we have, correct to $O(\delta_i)$,

$$\frac{x(x_i, t)}{x_i} = b(t) - D(t)\bar{\delta}_i(x_i) , \tag{5.5a}$$

$$a(x_i, t) = b(t) - D(t)\delta_i(x_i) , \tag{5.5b}$$

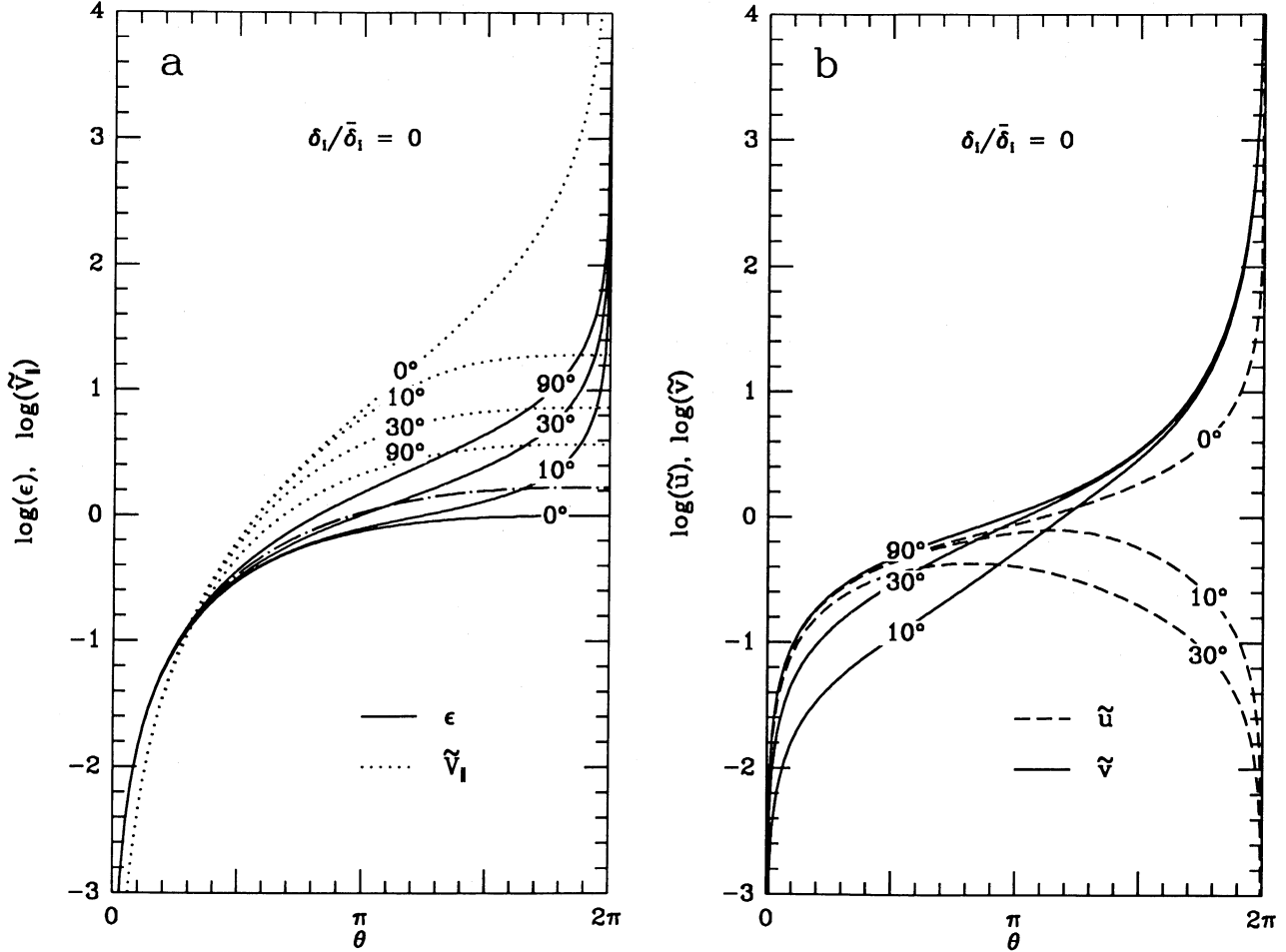$$\delta(x_i, t) = \frac{D(t)\delta_i(x_i)}{b(t) - D(t)\delta_i(x_i)} , \tag{5.5c}$$

FIG. 5.—Evolution of perturbations in spherical background flow for $\delta_i/\bar{\delta}_i = 0$. Coding to curves is same as in Fig. 2.

where we have used the definition (5.1a) and the relation $\rho/\rho_b = b(t)/(\partial x/\partial s)|_t$.

We now specialize to an $\Omega = 1$ cosmology, for which $\rho_b(t) = 1/6\pi G t^2$ and

$$b(t) = (t/t_i)^{2/3} . \tag{5.6a}$$

Then $D(t) = (t/t_i)^{4/3}$, and equations (5.5a)–(5.5c) become

$$x/x_i = (t/t_i)^{2/3}[1 - \bar{\delta}_i(t/t_i)^{2/3}] , \tag{5.6b}$$

$$a(t) = (t/t_i)^{2/3}[1 - \delta_i(t/t_i)^{2/3}] , \tag{5.6c}$$

$$\delta(t) = \frac{\delta_i(t/t_i)^{2/3}}{1 - \delta_i(t/t_i)^{2/3}} . \tag{5.6d}$$

In the linear regime ($\delta \ll 1$), equation (5.6d) reduces to the standard expression $\delta \approx \delta_i(t/t_i)^{2/3}$. The above equations show that particle separations in the y- and z-directions increase monotonically, while recollapse occurs in the x-direction. There are two different collapse times: x-separations of neighboring particles collapse to zero at time $t_c = t_i/\delta_i^{3/2}$ given by equation (5.6c), while a given mass plane passes through the symmetry plane $x = 0$ at time $t_s = t_i/\bar{\delta}_i^{3/2}$ given by equation (5.6b). The solution derived above assumes no crossing of mass planes, and so is valid up to time t_s at the latest. The condition that t_s increase with increasing s is $d\bar{\delta}_i/ds \leq 0$, which implies $\delta_i \leq \bar{\delta}_i$, and thus $t_c \geq t_s$.

b) Perturbation Equations

As in the case of spherical flow, we have two degenerate principal axes. Defining (u, v, w) to be the peculiar velocity components parallel to the (x, y, z) axes, the perturbation equations in the planar case are the same as equations (4.14)–(4.17) for the spherical case. We now convert to dimensionless variables analogous to those used in the spherical case. Define a new time variable θ by

$$t \equiv \frac{t_i}{\delta_i^{3/2}} \theta^3 \equiv \frac{t_i}{\delta_i^{3/2}} T(\theta) . \tag{5.7a}$$

The scale factors (eq. [5.6a], [5.6c]) can then be written as

$$a = \frac{1}{\delta_i} \theta^2(1 - \theta^2) \equiv \frac{1}{\delta_i} A(\theta) , \tag{5.7b}$$

$$b = \frac{1}{d_i} \theta^2 \equiv \frac{1}{\delta_i} B(\theta) . \tag{5.7c}$$

In terms of these new variables, the local expansion starts at $\theta = 0$, reaches a maximum in x at $\theta = 1/2^{1/2}$ and recollapses in x at $\theta = 1$. However, the above local behavior can only apply up to the time when the mass sheet passes through $x = 0$, which occurs at $\theta_s = \delta_i^{1/2}(t_s/t_i)^{1/3} = (\delta_i/\bar{\delta}_i)^{1/2} \leq 1$. As in the spherical case, we define an anisotropy factor

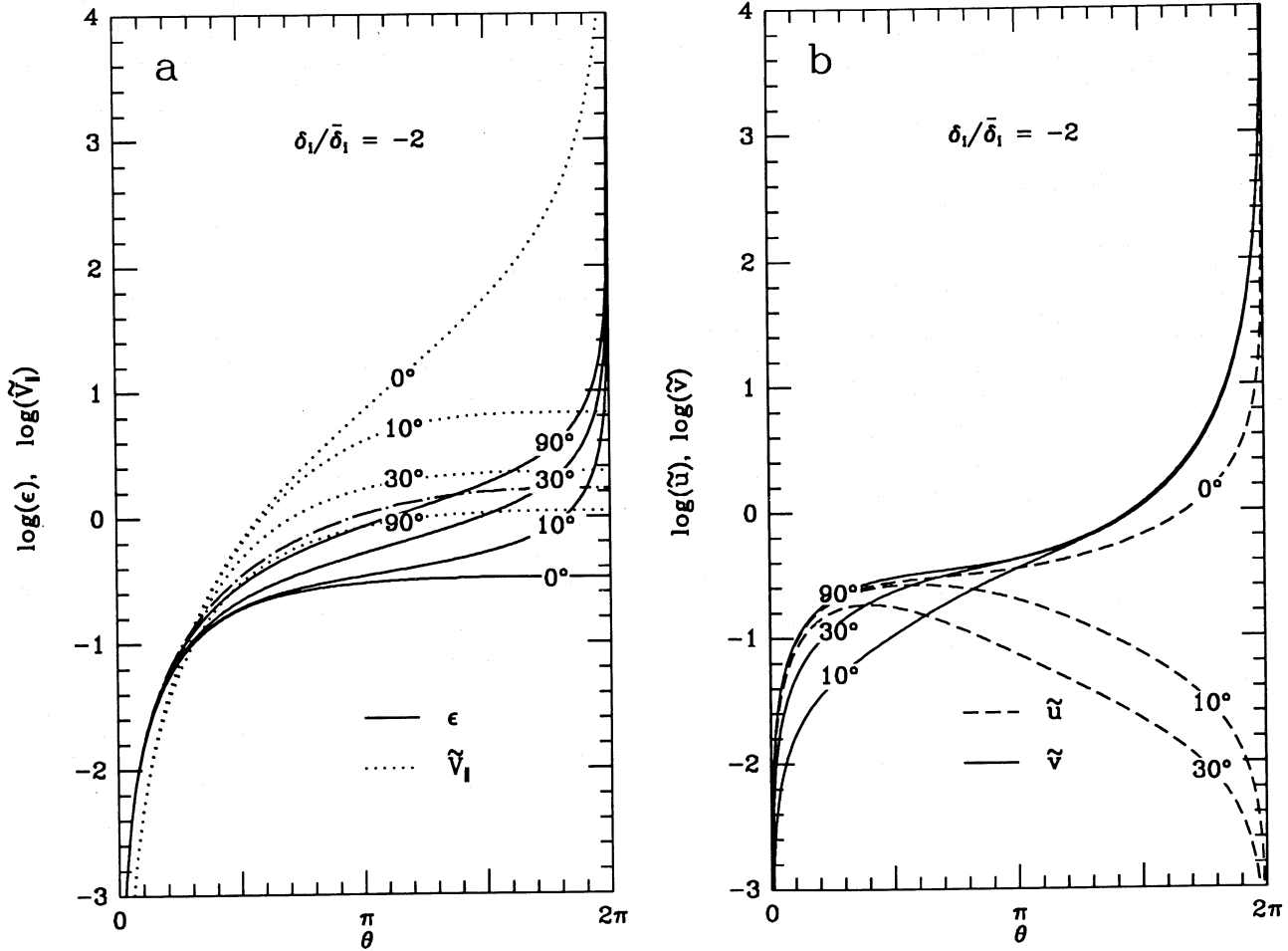$$F(\theta) \equiv A(\theta)/B(\theta) = 1 - \theta^2 . \tag{5.7d}$$

FIG. 6.—Evolution of perturbations in spherical background flow for $\delta_i/\bar{\delta}_i = -2$. Coding to curves is same as in Fig. 2.

The inclination of a perturbation evolves according to $\tan \beta = F(\theta) \tan \alpha$. $F \to 0$ as $\theta \to 1$, so that perturbations tend to align with their wavevectors parallel to the x-direction as the collapse proceeds. We also define

$$(\tilde{U}, \tilde{V}, \tilde{W}) \equiv -i\delta_i^{1/2} q t_i (U, V, W), \quad (5.8a)$$

$$(\tilde{u}, \tilde{v}, \tilde{w}) \equiv \left(\frac{\tilde{U}}{A}, \frac{\tilde{V}}{B}, \frac{\tilde{W}}{B}\right), \quad (5.8b)$$

$$Q^2 \equiv \delta_i^{3\gamma-4} \left(\frac{q}{q_{Ji}}\right)^2, \quad (5.8c)$$

$$\tilde{q} = q x_i, \quad (5.8d)$$

so that the peculiar velocity in physical units is

$$(u, v, w) = \left(\frac{\delta_i^{1/2} x_i}{t_i}\right) \frac{i}{\tilde{q}} (\tilde{u}, \tilde{v}, \tilde{w}). \quad (5.9)$$

Thus $\delta_i^{1/2} x_i/t_i$ is a characteristic velocity scale. The validity of the short-wavelength approximation requires $\tilde{q} \gg 1$. In terms of these new variables, the evolution equations for perturba-

tions become

$$\frac{d\epsilon}{d\theta} = \frac{3}{F^2 B} [(\cos^2 \alpha + F^2 \sin^2 \alpha) \tilde{V}_{\parallel}$$

$$+ \sin \alpha \cos \alpha (1 - F^2) \tilde{V}_{\perp}], \quad (5.10a)$$

$$\frac{d\tilde{V}_{\parallel}}{d\theta} = \frac{2F\epsilon}{(\cos^2 \alpha + F^2 \sin^2 \alpha)} \left[1 - \frac{Q^2(\cos^2 \alpha + F^2 \sin^2 \alpha)}{F^\gamma B^{3\gamma-4}}\right]. \quad (5.10b)$$

Note that in this form the perturbation equations are independent of the initial amplitude δ_i of the background perturbation. There are four independent modes: three of these may be taken to have $\tilde{W} = 0$; the evolution of the fourth, having $\epsilon = \tilde{U} = \tilde{V} = 0$ and $\tilde{W} \neq 0$ is trivial and will not be discussed further.

In general, complete solutions of the perturbation equations can be found only by numerical integration. However, for the special case that the perturbation has the same symmetry as the background solution (i.e., $\alpha = 0$) and pressure is negligible, one can derive an analytic solution. In this case, the density field is $\rho/\rho_b = (1 + \delta)(1 + \epsilon)$, and its evolution is given by equa-

tion (5.5c), with δ_i replaced by $\delta_i + \epsilon_i$, assuming $\delta_i, \epsilon_i \ll 1$. Substituting these definitions, and expanding to first order in ϵ, one finds

$$\epsilon \approx \epsilon_i \frac{D(t)/b(t)}{1 - \delta_i D(t)/b(t)} = \left(\frac{\epsilon_i}{\delta_i}\right)\delta = \left(\frac{\epsilon_i}{\delta_i}\right)\frac{\theta^2}{1 - \theta^2}, \quad (5.11)$$

where the last is for an $\Omega = 1$ cosmology.

c) Evolution of Perturbations with Zero Pressure: Asymptotic Analyses

We consider first the evolution of perturbations in the simple case that the effects of pressure can be neglected. The evolution of perturbations in the generic case $\alpha \neq 0, \pi/2$ is qualitatively as follows: as $\theta \to 0$, the expansion becomes isotropic, and there are growing, decaying, and vorticity modes whose form approaches that for the modes in an $\Omega = 1$ cosmology. The anisotropy of the local velocity field becomes significant for $\theta \gtrsim 1/2^{1/2}$ (corresponding to $F \lesssim \frac{1}{2}$), causing the wavevector to be sheared toward the x-direction, and the density perturbation associated with the vorticity mode to become significant. For $\theta \to 1$, $\beta \to 0$ for any perturbation with $\alpha \neq \pi/2$, and in the generic case, $\epsilon \to \infty$ and $\tilde{v}/\tilde{u} \to 0$.

i) Behavior for $\theta \to 0$

In the limit $t \to 0$, the scale factors have the dependence

$$t \propto T = \theta^3, \quad B = \theta^2, \quad F \sim 1. \quad (5.12)$$

There are two zero-vorticity modes, one growing and the other decaying. The growing mode has the behavior

$$\epsilon \sim \left(\frac{\epsilon_{i1}}{\delta_i}\right)\theta^2, \qquad \tilde{V}_\| \sim \frac{2}{3}\left(\frac{\epsilon_{i1}}{\delta_i}\right)\theta^3,$$

$$\tilde{u} \sim \frac{2}{3}\left(\frac{\epsilon_{i1}}{\delta_i}\right)\theta \cos \alpha, \quad \tilde{v} \sim \frac{2}{3}\left(\frac{\epsilon_{i1}}{\delta_i}\right)\theta \sin \alpha, \qquad (5.13)$$

while the decaying mode has behavior

$$\epsilon \sim (\epsilon_{i2}\delta_i^{3/2})\frac{1}{\theta^3}, \qquad \tilde{V}_\| \sim -(\epsilon_{i2}\delta_i^{3/2})\frac{1}{\theta^2},$$

$$\tilde{u} \sim -(\epsilon_{i2}\delta_i^{3/2})\frac{1}{\theta^4}\cos \alpha, \quad \tilde{v} \sim -(\epsilon_{i2}\delta_i^{3/2})\frac{1}{\theta^4}\sin \alpha, \qquad (5.14)$$

where ϵ_{i1} and ϵ_{i2} are the amplitudes of these modes at the time $\theta_i \ll 1$ when the background perturbation has amplitude $\delta_i \approx \theta_i^2$. The vorticity mode may be taken to have the form

$$\epsilon \sim -3\tilde{V}_\perp \sin \alpha \cos \alpha \theta, \quad \tilde{V}_\| \sim -3\tilde{V}_\perp \sin \alpha \cos \alpha \theta^2,$$

$$\tilde{u} \sim \frac{\tilde{V}_\perp \sin \alpha}{\theta^2}, \qquad \tilde{v} \sim -\frac{\tilde{V}_\perp \cos \alpha}{\theta^2}. \qquad (5.15)$$

The asymptotic behavior of the density modes is the same as one derives for an $\Omega = 1$ cosmology.

ii) Behavior for $\theta \to 1$ ($\alpha \neq \pi/2$)

Expanding in powers of $\eta \equiv 1 - \theta$, we find that in the limit $t \to t_c$, the scale factors have asymptotic dependence

$$t_c - t \propto 1 - T \sim 3\eta, \quad B \sim 1, \quad F \sim 2\eta \propto t_c - t, \quad (5.16)$$

so that the background density has the dependence $\rho \propto \eta^{-1} \propto (t_c - t)^{-1}$. This limiting behavior of the expansion factors with time is the same as one finds for any gravitational collapse in which one axis contracts to zero while the other two axes

remain finite (for instance, generic collapse of a homogeneous spheroid gives the same result). There are two independent zero-vorticity solutions, one growing as $\eta \to 0$:

$$\epsilon \sim \frac{c_1}{\eta}, \qquad \tilde{V}_\| \sim \frac{4}{3}c_1 \sec^2 \alpha,$$

$$\tilde{u} \sim \frac{2}{3}c_1 \sec \alpha \frac{1}{\eta}, \qquad \tilde{v} \sim \frac{4}{3}c_1 \sec \alpha \tan \alpha, \qquad (5.17)$$

and the other neutral as $\eta \to 0$:

$$\epsilon \sim c_2, \qquad \tilde{V}_\| \sim -2c_2 \sec^2 \alpha \eta^2,$$

$$\tilde{u} \sim -c_2 \sec \alpha \eta, \quad \tilde{v} \sim -2c_2 \sec \alpha \tan \alpha \eta^2. \qquad (5.18)$$

There is a third independent solution having nonzero vorticity:

$$\epsilon \sim 3\tilde{V}_\perp \tan \alpha \eta, \qquad \tilde{V}_\| \sim -\tilde{V}_\perp \tan \alpha,$$

$$\tilde{u} \sim -2\tilde{V}_\perp \sec \alpha \tan \alpha \eta^2, \quad \tilde{v} \sim -\tilde{V}_\perp \sec \alpha. \qquad (5.19)$$

The behavior of the zero-vorticity solutions is exactly the same as one derives from the analysis of § III for a purely radial perturbation (case [a(i)], $\alpha_1 = \beta = 1$), with density growth being driven by kinematics rather than self-gravity. We see that a generic perturbation has density growing as $\epsilon \propto (t_c - t)^{-1}$ as the singularity is approached.

iii) Behavior as $\theta \to 1$ ($\alpha = \pi/2$)

For the special case that the wavevector is initially exactly tangential, it remains tangential, and the perturbation behavior as $t \to t_c$ is different from the generic case. Of the two zero-vorticity modes, one is neutral as $\eta \to 0$:

$$\epsilon \sim c_1, \quad \tilde{V}_\| \sim -c_1 \ln \eta,$$

$$\tilde{u} = 0, \qquad \tilde{v} \sim -c_1 \ln \eta, \qquad (5.20)$$

while the other is decaying:

$$\epsilon \sim c_2 \eta, \quad \tilde{V}_\| \sim -\tfrac{1}{3}c_2,$$

$$\tilde{u} = 0, \qquad \tilde{v} \sim -\tfrac{1}{3}c_2. \qquad (5.21)$$

The vorticity mode has dependence:

$$\epsilon = 0, \quad \tilde{V}_\| = 0,$$

$$\tilde{u} \sim \frac{\tilde{V}_\perp}{2\eta}, \qquad \tilde{v} = 0. \qquad (5.22)$$

The behavior of the zero-vorticity modes cannot be derived directly from the analysis of § III, because $\alpha_1 = 0$, $B = 1$ for a purely tangential perturbation (see case [a(i)]). A careful analysis shows that density growth in this case is driven by self-gravity.

d) Perturbation Evolution with Zero Pressure: Numerical Integrations

Complete solutions for perturbation growth with zero pressure in the general case are obtained by numerical integration of the equations, with initial conditions given by one of the $\theta \to 0$ asymptotic solutions (5.13), (5.14), (5.15). In the cosmological case, growing mode initial conditions are of the most interest, so we give numerical results only for this case, normalized to $\epsilon_i/\delta_i = 1$. Figure 7 gives ϵ, $\tilde{V}_\|$, $\tilde{u}$, and $\tilde{v}$ as functions of θ for $\alpha = (0°, 60°, 80°, 90°)$, together with the $\theta \to 0$ asymptote to ϵ given by equation (5.13). Note that the $\theta \to 0$ asymptote is exactly the same as the behavior in an unperturbed $\Omega = 1$ background, so that it is convenient to take this as a standard
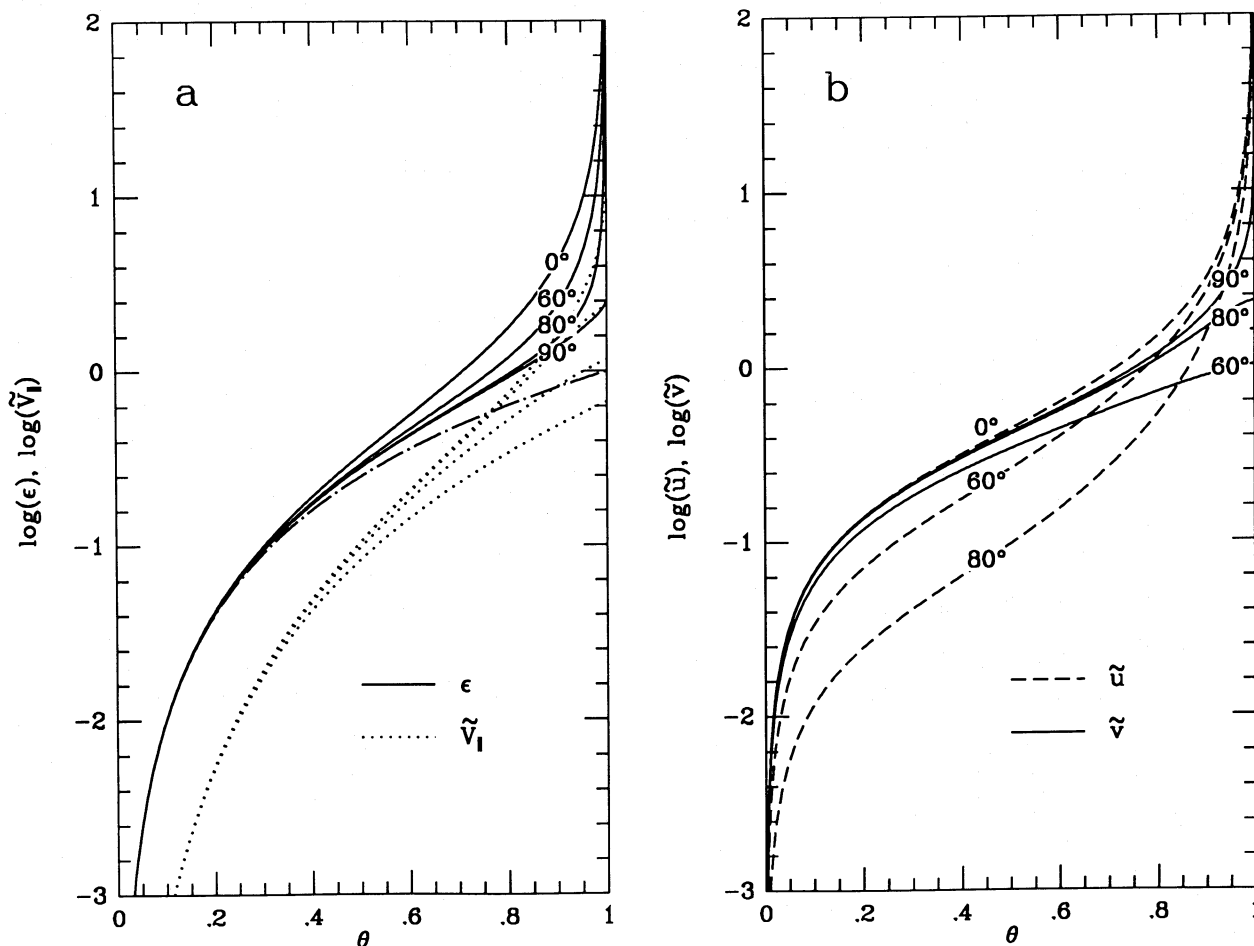
Fig. 7.—Evolution of perturbations in planar background flow, for inclination angle $\alpha = (0°, 60°, 80°, 90°)$. (a) ϵ and $\tilde{V}_\parallel$, together with evolution of ϵ in an $\Omega = 1$ cosmological model (*dot-dash curve*). (b) $\tilde{u}$ and $\tilde{v}$. Curves are labeled by value of α. (Labeling on $\tilde{V}_\parallel$ curves suppressed for clarity; it runs in the opposite sense vertically to that on ϵ curves.)

case for comparison purposes. The perturbation growth begins to exceed the standard case once the local expansion differs significantly from that of an $\Omega = 1$ cosmology, which occurs for $\theta \gtrsim 1/2^{1/2}$. For an exactly tangential perturbation ($\alpha = \pi/2$), the growth rate at given θ is larger only because the local density is larger (by a factor $b/a = 1/F$). For a radial perturbation ($\alpha = 0$), the growth is boosted also because the local velocity field changes from expansion to contraction along the direction of the wavevector, and this is the dominant effect as $\theta \to 1$. Perturbations with intermediate inclinations have intermediate behavior. For $\alpha \gtrsim 1$, the perturbation growth at first approximates that for $\alpha = \pi/2$, until the wavevector is sheared around to being nearly radial, which occurs for $F \tan \alpha \lesssim 1$, after which the growth tracks that for $\alpha = 0$.

e) Perturbation Evolution with Pressure

One can obtain the effects of pressure on the limiting evolution of density perturbations as $t \to t_c$ using the analysis of § III. For the generic case $\alpha \neq \pi/2$, a perturbation becomes radial in this limit, and we have $\alpha_1 = 1$, $\beta = 1$. Then we have case (b), in which pressure dominates self-gravity in the limit, provided $\gamma > 0$. For $0 < \gamma < 1$ (case [b(i)]), kinematics dominates pressure as $t \to t_c$, so that perturbations have the same limiting behavior (with a growing and a neutral solution) as for $p = 0$. For $\gamma > 1$ (case [b(iii)]), pressure dominates over kine-

matics, leading to rapid oscillations in ϵ, with oscillation amplitude varying as $\epsilon \propto (t_c - t)^{-(3-\gamma)/4}$. $\gamma = 1$ (case [b(ii)]) is an intermediate case. Analysis based on equations (5.10a) and (5.10b) shows that for $Q < 1/6^{1/2}$, there are two power-law solutions, both growing more slowly than for $p = 0$, while for $Q > 1/6^{1/2}$, there are oscillatory solutions with oscillation amplitude growing as $\epsilon \propto (t_c - t)^{-1/2}$. For the special case $\alpha = \pi/2$ of an exactly tangential perturbation, pressure is negligible compared to self-gravity as $t \to t_c$ for $\gamma < 2$ (case [a]), so that the limiting evolution is the same as for $p = 0$.

The full evolution including pressure can be found only by integrating the equations numerically. Pressure will cause the perturbation to have oscillatory or growing behavior around the time when the background perturbation turns around at $\theta = 1/2^{1/2}$ according as $Q \gtrsim 1$ or $Q \lesssim 1$. At later times, the relative importance of pressure increases or decreases depending on the value of γ and the orientation α, as described above.

VI. DISCUSSION OF RESULTS FOR THREE-DIMENSIONAL FLOWS

a) Comparison with Previous Work

There has been some previous work on perturbation growth in inhomogeneous flows having spherical symmetry. McNally and Settle (1980) investigated the evolution in the linear regime of *radial* perturbations in inhomogeneous pressure-free spher-

ical flows, without making any short-wavelength assumption. They show how the general solution for the evolution of pressure-free perturbations in any such flow may be obtained by quadratures, and derive analytical expressions for two particular cases, although not for the case of cosmological initial conditions. The limiting behavior of perturbations they find as collapse is approached is identical to that found here. However, they go on to draw conclusions about the evolution of perturbations in general that are not justified, since, as we have shown, the radial case is very special. As already mentioned, Ryden and Gunn (1987) derived an expression for the growing mode for radial perturbations of a pressure-free background collapse corresponding to cosmological initial conditions, effectively in the short-wavelength limit, which agrees with the results of this paper. The growth of density perturbations in inhomogeneous spherical collapse has also been investigated by Arny (1966) using a particle method whose precise validity is difficult to judge. He considers small-scale *ellipsoidal* perturbations, but does not study the effects of perturbation orientation. The results he obtains on the effects of central concentration on perturbation growth agree qualitatively with those found here, but he gives too few details of his calculations for a quantitative comparison to be possible.

A paper on a somewhat related subject has recently been published by Aarseth, Lin, and Papaloizou (1988). They present a new derivation of the results of Hunter (1962, 1964) for perturbations in a pressure-free, homogeneous spherical collapse. Their results for "internal modes" are equivalent to those given in § IVc(iv). They also show how the same results apply to the homogeneous core of an inhomogeneous spherical collapse, but give no analysis of how perturbations evolve in the regions of the flow where density gradients are significant. They apply these results to an analysis of the collapse and violent relaxation of a protoglobular cluster, represented by a system of point particles. Their *N*-body results demonstrate the importance of the growth of density perturbations for the generation of random velocities which eventually halts the collapse. In their paper, Aarseth *et al.* distinguish between "local" fluctuations due to discrete particle effects, and "global" fluctuations on scales involving many particles. In the present paper, the fluid is treated as a continuum, so there are only "global" fluctuations. Aarseth *et al.* concentrate on the case that the initial rms density fluctuations vary with mass M as $\langle (\delta\rho/\rho)^2 \rangle^{1/2} \propto M^{-1/2}$, but this is fairly arbitrary, and one could equally well consider different perturbation spectra.

There has also been some work on growth of density perturbations in collapsing uniform density spheroids, for which the behavior is analogous to that in the plane-symmetric collapses considered in this paper. Falle (1972) derived an equation for perturbations in a nonrotating oblate spheroid of the same form as equation (2.34). He incorrectly argued from this that density perturbations which are prolate relative to the background flow would grow fastest. Silk (1982) investigated evolution of ellipsoidal perturbations concentric with a nonrotating oblate ellipsoidal background flow and found that the fastest growing perturbations are those which are oblate relative to the background flow, in agreement with the results found here. He also derives expressions for the limiting behavior of perturbations as the pancake collapse is approached; he finds the correct growing mode solution for the case that the wavevector is perpendicular to the pancake plane, but finds only the decaying mode for case that it is parallel. There has also been some work on perturbations in rotating oblate spheroids by Arny

(1967), but he does not consider the nonrotating limit, so his results cannot be directly compared with those found here. Equations (8) and (9) of his paper imply that evolution is independent of the orientation of the perturbation, but contain an error: the factor l/m should be l/mK_4^2, where the separation constant K_4 contains the information about the orientation.

b) Implications for Nonlinear Evolution

A common feature of the pressure-free inhomogeneous spherically symmetric and plane symmetric background collapses studied in the previous sections is that at late stages of the collapse, when the local velocity field around any point has become significantly anisotropic, growth of density perturbations is dominated by the kinematic effects of the background flow rather than by the self-gravity of the perturbation. Homogeneous spherical background collapses, in which the effects on perturbation growth of self-gravity and kinematics are at all stages comparable, are completely atypical in this regard. As a consequence, perturbation growth during the later stages of these more general collapses is significantly anisotropic: if a perturbation is decomposed into plane waves, growth is fastest for those Fourier components having wavevectors aligned with that principal axis of the local velocity field along which contraction is the fastest (most negative $\dot{a}_i/a_i$). It seems likely that these conclusions will also apply to a generic inhomogeneous low-pressure collapse having no special symmetry, in which the scale factors along all three principal axes of the local flow are different. The importance of kinematic effects for perturbation growth in anisotropic flows was earlier noted by Zel'dovich and Novikov (1978, § 20.4) in the context of homogeneous anisotropic cosmological models. For such models, the global dynamics are given by general relativity, but the local dynamics of short-wavelength perturbations can be analyzed using Newtonian mechanics.

These ideas have important implications for the nonlinear evolution of density perturbations in a generic collapse. Consider the general case, for which the local flow has a unique fastest contracting principal axis. Assuming that the initial conditions on the perturbations on the average define no preferred directions (Fourier components drawn from a distribution which is statistically isotropic), then in the linear regime perturbation velocities will tend to become largest parallel to this principal axis, and the density field will develop peaks and troughs which are flattened perpendicular to this axis. It seems clear that the nonlinear evolution will consist of collapse down to planar configurations ("pancakes") aligned perpendicular to the fastest contracting axis. The evolution subsequent to the initial collapse depends on whether the matter involved is collisional or collisionless. For a collisional fluid, oppositely moving gas streams will collide (and presumably form shocks) at the midplane, resulting in a dense sheet of gas at that location. For a collisionless, fluid, the opposing streams of particles will pass through each other at the midplane, and the entire pancake may only have a fairly transient existence before the structure is erased by free streaming. In either case, the pancake when it forms should still be approximately comoving with the background flow in the transverse directions, since the Fourier components in the lateral directions having the same comoving wavelength $2\pi/q$ as the components along the collapse axis which are just going nonlinear should still be in the linear regime.

The above discussion may require modification if the background flow has some special symmetry, so that the scale

factors are equal along two degenerate principal axes. If the third, nondegenerate axis has the fastest contraction rate, as in the planar background collapses analyzed in § V, then there is a unique collapse axis for perturbations as before. However, if the nondegenerate axis has the slowest contraction rate, as for the spherical background collapses discussed in § IV, perturbation growth favors equally any Fourier component with wavevector in the *plane* containing the two degenerate axes. Even for statistically isotropic initial conditions on the perturbations, any given density peak will not be exactly spherical, so it is likely to collapse first along some particular axis lying in this degenerate plane, as determined by the peak's shape. However, the planar nature of the collapse will be less than for the case of a unique fastest contracting principal axis, and the collapse axes of different peaks will point in different (random) directions within the degenerate plane. The pancakes thus formed may subsequently collapse in one transverse direction to give filaments aligned along the slowest contracting principal axis.

It is worthwhile at this point to discuss the relation between this analysis and that of Zel'dovich (1970), which is also marked by the importance of kinematic effects and likewise predicts the formation of "pancakes." Zel'dovich takes the expression for the Lagrangian displacement of a particle derived from linear perturbation theory in a homogeneous, *isotropic*, expanding background, and extrapolates it into the *nonlinear* regime. This predicts that the initial stages of collapse for density perturbations with isotropic Gaussian random initial conditions will generically be planar. This result is closely related to the flattening instability for the collapse of homogeneous ellipsoids found by Lin, Mestel, and Shu (1965): a generic peak in such a density field is significantly triaxial, and the *self-gravity* of the perturbation, which in this case is important in driving density growth in the linear regime, generates a triaxial velocity field, which causes collapse to occur first along the shortest axis. The later stages of the collapse are essentially kinematic, with particles accelerated only to finite velocities, which is the reason why this extrapolation of linear theory is a good approximation in the general case. The method is much less accurate if applied to the collapse of a spherical peak, since then gravitational accelerations diverge as the peak collapses. In contrast, in the analysis in the present paper, anisotropic evolution of density perturbations already arises in the *linear* regime, as a result of the dominance of *kinematic* effects over self-gravity, in a background flow which is *anisotropic*. The background flow, even if initiated from a density perturbation in an isotropic cosmological model, might be very poorly described by the Zel'dovich approximation, so that the Zel'dovich approximation could not be directly applied to predict the pancaking of small-scale structure. The pancakes predicted in an anisotropic background flow have preferred orientations fixed by the flow, while the pancakes predicted in an isotropic background flow by the Zel'dovich analysis do not.

The discussion given here of nonlinear evolution of perturbations in anisotropic background flows only strictly applies to the first scales to collapse (the same remark also applies to the Zel'dovich analysis). Suppose there is initially a spectrum of density perturbations of different wavelengths, with the rms amplitude having a peak at a certain wavelength. Then collapse will occur first on the scale corresponding to this peak, and will proceed as already described. The evolution of perturbations on larger scales in the linear regime should not be

much affected by the nonlinear evolution on small scales, at least insofar as pressure is unimportant. However, the clumping and peculiar velocities due to collapse on small scales will tend to disrupt the formation of well defined pancakes by the nonlinear collapse of larger scales, although some remnant of pancake structure is likely to remain.

VII. PERTURBATION GROWTH IN A PLANAR SHEET

In this section, we analyze perturbation growth in a planar fluid sheet which is undergoing anisotropic expansion or contraction in its own plane. This is the two-dimensional analog of the three-dimensional problem considered in previous sections of this paper. A principal motivation for this analysis is the inference that the nonlinear evolution of perturbations in anisotropic background flows is likely to consist of collapse down to a planar sheet or pancake of gas (we consider here only the case of a collisional fluid). The properties of the first pancakes to form can be estimated as follows: suppose that collapse occurs along the z-axis, for perturbations having comoving wavenumber q_3. Collapse occurs when linear theory predicts a relative overdensity $\epsilon \simeq 1$, and a peculiar velocity parallel to the wavevector $v_\parallel$. The wavelength in the collapse direction is $\lambda_3 = 2\pi a_3/q_3$, and all fluid within distance $\pm \lambda_3/2$ of the midplane of the perturbation collapses down to form a sheet of surface density $\sigma = \rho_b \lambda_3$, ρ_b being the background density at that time. For a collisional fluid, the kinetic energy in the collapse motions ends up being thermalized, resulting in a sound speed in the pancake layer $c_s \simeq v_\parallel$ if there are no energy losses, with smaller values if radiative cooling is significant. We assume that the vertical collapse is completed and the fluid sheet reaches approximate dynamical equilibrium in the vertical direction, with thickness h, while in the transverse directions it is still approximately comoving with the background flow. The transverse extent of the fluid sheet is expected to be at least $L_1 \gtrsim 2\pi a_1/q_3$, $L_2 \gtrsim 2\pi a_2/q_3$ in the x, y directions, respectively. We assume that the sheet is "thin," with $h \ll (L_1, L_2)$. Then for perturbations within the sheet having wavelengths $\lambda \gg h$, the behavior of the sheet can be approximated as being two-dimensional. This is the basic simplifying assumption made in the rest of this section.

a) Perturbation Equations in a Two-dimensional Sheet

We consider perturbations to a fluid layer in the thin sheet approximation: The layer is assumed to be symmetric about the plane $z = 0$, and to be locally self-gravitating and in hydrostatic equilibrium in the z-direction at all times, with local thickness h. In addition, the z-dependence of the horizontal velocity and the horizontal gravitational force is assumed to be ignorable. Under these circumstances, the z-dependence of the equations of motion can be integrated out, and the equations effectively become two-dimensional. This approximation becomes rigorous for variations with horizontal wavelengths $\lambda \gg h$ (e.g., Goldreich and Lynden-Bell 1965), but gives useful answers even for $\lambda < h$. The thin sheet approximation has been used extensively in studies of the dynamics of galactic disks (e.g., see Hunter 1983 for a review), and has also been applied by Tomisaka and Ikeuchi (1985) to an investigation of perturbation growth in an isotropically expanding fluid sheet. Here I extend this analysis to the case of anisotropic expansion/contraction.

We define ρ and p to be the volume density and three-dimensional pressure within the sheet, and define a surface

density and integrated pressure by integrating over the vertical extent of the sheet:

$$\sigma \equiv \int_{-\infty}^{\infty} \rho \, dz \quad \text{and} \quad P \equiv \int_{-\infty}^{\infty} p \, dz .$$

We define u to be the velocity parallel to the plane of the sheet. With the assumptions listed above, the z-integrated continuity and Euler equations, together with the Poisson equation, are (see eqs. [2.1], [2.2], [2.3])

$$\frac{D\sigma}{Dt} = -\sigma \nabla_{\|x} \cdot u , \qquad (7.1a)$$

$$\frac{Du}{Dt} = -\nabla_{\|x} \Phi|_{z=0} - \frac{1}{\sigma} \nabla_{\|x} P , \qquad (7.1b)$$

$$\nabla^2 \Phi = 4\pi G \rho , \qquad (7.1c)$$

where $\nabla_{\|}$ is the component of the gradient operator parallel to the sheet, and D/Dt is the time derivative comoving with the two-dimensional velocity u. The source term for Φ in equation (7.1c) may include contributions from mass external to the sheet. The integrated pressure is assumed to be uniquely related to the surface density, $P = P(\sigma)$, so that it is derivable from a two-dimensional enthalpy

$$H(\sigma) = \int dP/\sigma = \int C_s^2 \, d\sigma/\sigma ,$$

where $C_s = (dP/d\sigma)^{1/2}$ is the two-dimensional sound speed. If the three-dimensional pressure is given by the relation $p \propto \rho^\gamma$, then, as is shown in Appendix A, the two-dimensional pressure is given by $P \propto \sigma^\Gamma$, where the polytropic indices are related by $\Gamma = 3 - 2/\gamma$. Thus, the physically interesting range $1 \le \gamma \le 5/3$ corresponds to $1 \le \Gamma \le 9/5$. As in the three-dimensional case, the vorticity obeys a conservation law; in the two-dimensional case, only the z-component of the vorticity is interesting.

The method followed for analyzing perturbations in a two-dimensional flow is essentially the same as that for a three-dimensional flow as presented in § II, so we just summarize the derivation here. We consider a background flow which varies on scale L parallel to the plane of the sheet, and perturbations to this flow having wavelength $\lambda \ll L$. We introduce coordinates X_i ($i = 1, 2$) comoving with the background flow in the plane of the sheet, and define scale factors $A_{ij}(t) = (\partial x_i/\partial X_j)|_t$ as before. The local background flow around a point comoving with the fluid can be approximated by a linear velocity field $u'_{bi} = H_{ij} x'_j$ and a constant surface density $\sigma_b = \sigma_0$. We now consider a perturbed motion of the form $\sigma = \sigma_b(1 + \epsilon)$, $u' = u'_b + v$, $\Phi = \Phi_b + \chi$. After linearizing in perturbed quantities and discarding terms $O(x'/L)$, $O(\lambda/L)$, we obtain the perturbation equations

$$\left.\frac{\partial \epsilon}{\partial t}\right|_{X'} = -A_{ji}^{-1} \frac{\partial v_i}{\partial X'_j} , \qquad (7.2a)$$

$$\left.\frac{\partial v_i}{\partial t}\right|_{X'} + H_{ij} v_j = -A_{ji}^{-1} \frac{\partial}{\partial X'_j} (\chi|_{z=0} + C_s^2 \epsilon) , \qquad (7.2b)$$

$$A_{ji}^{-1} A_{ki}^{-1} \frac{\partial^2 \chi}{\partial X'_j \partial X'_k} + \frac{\partial^2 \chi}{\partial z^2} = 4\pi G \sigma_0 \epsilon \delta(z) , \qquad (7.2c)$$

where the summation convention is assumed and the index i runs over values $i = 1, 2$. In equation (7.2c), we have

assumed that the perturbed gravitational field is due only to density perturbations within the sheet, which is treated as having infinitesimal vertical thickness. As in the three-dimensional case, we specialize to a background flow having zero vorticity, $\nabla_{\|x} \wedge u_b = 0$, and the perturbation equations can be simplified by introducing the new velocity variable $V_i \equiv A_{ji} v_j$. We consider plane-wave perturbations, having spatial dependence of the form $\exp (iq \cdot X') = \exp (ik \cdot x')$, where q and k have components only in the plane of the sheet. Substituting into the perturbation equations, one finds that the perturbed Poisson equation (7.2c) has the solution

$$\chi|_{z=0} = -\frac{2\pi G \sigma_0 \epsilon}{(P_{ij} q_i q_j)^{1/2}} , \qquad (7.3)$$

where $P_{ij} = A_{ik}^{-1} A_{jk}^{-1}$. As in the three-dimensional case, we separate V into components parallel and perpendicular to q, and the perpendicular component $V_\perp$ is constant with time because of vorticity conservation. Combining equations (7.2b) and (7.3), we obtain an equation for the parallel component $V_\|$

$$\frac{dV_\|}{dt} = iq \left[\frac{2\pi G \sigma_0}{(P_{ij} q_i q_j)^{1/2}} - C_s^2 \right] \epsilon , \qquad (7.4)$$

while equation (7.2a) gives an equation for ϵ

$$\frac{d\epsilon}{dt} = -iP_{ij} q_i \left(q_j \frac{V_\|}{q} + V_{\perp j} \right) . \qquad (7.5)$$

These two equations can be combined into a single equation for the evolution of the density perturbation:

$$\frac{d^2\epsilon}{dt^2} - 2 \frac{\dot{k}}{k} \frac{d\epsilon}{dt} + (C_s^2 k^2 - 2\pi G \sigma_0 k)\epsilon$$
$$= -i \left(\dot{P}_{ij} - 2\frac{\dot{k}}{k} P_{ij} \right) q_i V_{\perp j} , \qquad (7.6)$$

where $k^2 = P_{ij} q_i q_j$ as before. This is identical to the corresponding equation (2.32b) for the three-dimensional case, except that the effect of self-gravity is given by a term $2\pi G \sigma_0 k$ rather than $4\pi G \rho_0$. This has the important consequence that for perturbations in which the effect of pressure is negligible compared to self-gravity and background kinematics, the growth rate is larger for smaller wavelengths, in contrast to the three-dimensional case, in which it is the same for all wavelengths. The critical Jeans wavevector for which pressure exactly balances self-gravity is $k_J = 2\pi G \sigma_0 / C_s^2 = (2/\Gamma I_y)(1/h)$, where h is the half-thickness of the layer derived in Appendix A. The thin sheet approximation made here is strictly valid only for $kh \ll 1$; however, comparison of results derived with and without the thin sheet approximation for other analogous problems (e.g., Larson 1985) suggests that this approximation gives answers correct to factors of order unity even for $kh > 1$. Equation (7.6) simplifies considerably if the shear flow has fixed principal axes, $A_{ij}(t) = \text{diag} [a_1(t), a_2(t)]$, and if we consider perturbations aligned with one of the principal axes, say $q = (q_1, 0)$. Then

$$\frac{d^2\epsilon}{dt^2} + 2 \frac{\dot{a}_1}{a_1} \frac{d\epsilon}{dt} + \left[C_s^2 \left(\frac{q_1}{a_1} \right)^2 - 2\pi G \sigma_0 \left(\frac{q_1}{a_1} \right) \right] \epsilon = 0 . \qquad (7.7)$$

This equation is equivalent to equation (4.10) of Tomisaka and Ikeuchi (1985), derived for an isotropically expanding/contracting sheet.

b) General Behavior of Perturbations

The evolution of perturbations in a two-dimensional flow can be analyzed in a similar manner to that for the three-dimensional case. Henceforth, we concentrate on vorticity-free perturbations ($V_\perp = 0$), since these seem to be of the most interest in practice. The type of behavior depends on the wavenumber; for simplicity of exposition, consider a perturbation aligned with a principal axis, so that $k = q_1/a_1$. If $k_J C_s = 2\pi G\sigma/C_s \gtrsim \dot{a}_1/a_1$, there are three regimes to consider. For $k \gg k_J$, the pressure term dominates in equation (7.7), and ϵ oscillates as a sound wave. For $k_J \gg k \gg (1/2\pi G\sigma)(\dot{a}_1/a_1)^2$, self-gravity dominates, and ϵ has growing and decaying solutions. For $k \ll (1/2\pi G\sigma)(\dot{a}_1/a_1)^2$, the kinematic term dominates, and the growth of ϵ is exactly the same as it would be in the three-dimensional case with the same scale factor $a_1(t)$. If $k_J C_s \lesssim \dot{a}_1/a_1$, then the intermediate range of k in which self-gravity dominates disappears. For a sheet formed by pancake collapse in a three-dimensional anisotropic background flow, we take the transverse scale factors in the sheet to be the same as $a_1(t)$, $a_2(t)$ for the three-dimensional flow. Then the condition on the wavelength for self-gravity to dominate can also be written as $h \ll \lambda_1 \ll [4\pi^2 G\rho_b/(\dot{a}_1/a_1)^2]\lambda_3$. The transverse extent of the sheet in the x_1-direction is $L_1 \gtrsim (a_1/a_3)\lambda_3$. Now $a_1/a_3 \geq 1$ (since the z-axis in the three-dimensional flow is assumed to be the fastest contracting), and in practice (see §§ IV and V) we find typically $4\pi G\rho_b/(\dot{a}_1/a_1)^2 \lesssim 1$, so a necessary condition for self-gravity to dominate is $h \ll \lambda_1 \ll L_1$, i.e., the sheet must be thin.

While the perturbation equations can be solved exactly by numerical integration, given the time-dependence of the scale factors $a_1(t)$, $a_2(t)$, it is useful to consider approximate methods of solution. We rewrite equation (7.6) (for $V_\perp = 0$) as

$$\frac{d^2\epsilon}{dt^2} - 2\frac{\dot{k}}{k}\frac{d\epsilon}{dt} = \omega^2\epsilon , \tag{7.8a}$$

where

$$\omega^2(t) = 2\pi G\sigma(t)k(t) - C_s^2(t)k^2(t) , \tag{7.8b}$$

and $k(t)$ is the proper wavenumber as before. Note that this form applies for arbitrary orientation of the wavevector. If ω is "large," then this equation may be solved by the WKB approximation. In Appendix B, we show that the WKB solutions have the form

$$\epsilon \approx c_\pm \frac{k(t)}{\sqrt{\omega(t)}} \exp\left[\pm \int \omega(t)dt\right], \tag{7.9a}$$

where the conditions for the approximation to be valid are roughly

$$\left|\frac{\dot{\omega}}{\omega^2}\right| \ll 1 , \quad \left|\frac{\dot{k}}{k\omega}\right| \ll 1 . \tag{7.9b}$$

Now $|\dot{k}/k| \simeq |\dot{a}_1/a_1|$ or $|\dot{a}_2/a_2|$, while typically $|\dot{\omega}/\omega| \simeq |\dot{a}_1/a_1|$, $|\dot{a}_2/a_2|$, so that the WKB validity conditions become $\omega \gg |\dot{a}_1/a_1|$, $|\dot{a}_2/a_2|$. For the perturbations with $k < k_J$ which grow due to self-gravity, the growth rate is maximized at wavenumber $k = \frac{1}{2}k_J$, for which $\omega = \frac{1}{2}C_s k_J$. Similar WKB treatments have been derived by Tomisaka and Ikeuchi (1985) and by Balbus (1988a) for the case of a shearing, rotating sheet.

In the opposite limit $\omega \ll |\dot{k}/k|$, we obtain an approximate solution by setting the right-hand side of equation (7.8a) to

zero. The equation may then be integrated to give

$$\epsilon \approx c_1 \int k^2(t)dt + c_2 . \tag{7.10}$$

The WKB method can also be applied to perturbations of three-dimensional flows, but in that case it is not useful for describing the growth of perturbations due to self-gravity. In the three-dimensional case, the perturbation equation takes the form of equation (7.8a), with $\omega^2(t) = 4\pi G\rho_b(t) - c_s^2(t)k^2(t)$. Therefore, for perturbations in which pressure dominates self-gravity, $\omega \approx ic_s k$, so the WKB validity conditions are fulfilled in any background flow for sufficiently large k. Thus sound waves can be described by WKB solutions. However, when self-gravity dominates pressure, $\omega \approx (4\pi G\rho_b)^{1/2}$, and these solutions could only be described by the WKB approximation if the condition $(4\pi G\rho_b)^{1/2}/(\dot{a}/a) \gg 1$ were satisfied, whereas for the background flows studied in this paper we have instead $(4\pi G\rho_b)^{1/2}/(\dot{a}/a) \lesssim 1$ except close to the turnaround time for a principal axis (in fact, this ratio tends to 0 as $t \to t_c$ for generic spherical and planar collapses). In contrast, for two-dimensional flows, when self-gravity dominates pressure, we have $\omega \approx (2\pi G\sigma k)^{1/2} = [(4\pi^2 G\rho_b)(a_3/a_1)(q_1/q_3)]^{1/2}$, and in this expression the factor $(q_1/q_3) \gtrsim 1$ can function as a large parameter and make the WKB approximation valid.

c) Power-Law Scale Factors

In analogy with the three-dimensional case, we can also study the limiting behavior of density perturbations aligned with a principal axis when $A_{ij}(t) = \text{diag}[a_1(t), a_2(t)]$ and the scale factors have power-law time dependence. Thus, we take a reference time t_i at which $a_i(t_i) = 1$ ($i = 1, 2$), $q_{1J}(t_i) = q_{1Ji}$ and $\sigma(t_i) = \sigma_i$ and introduce a dimensionless time variable $\tau = (2\pi G\sigma_i q_1)^{1/2}|t - t_c|$. We assume that the scale factors have time dependence $a_i(\tau) = (\tau/\tau_i)^{\alpha_i}$ ($i = 1, 2$), and define $\beta = \alpha_1 + \alpha_2$. (We assume $\beta > 0$ and $\alpha_1 \neq 0$.) Then, in terms of these variables, equation (7.7) becomes

$$\frac{d^2\epsilon}{d\tau^2} + \frac{2\alpha_1}{\tau}\frac{d\epsilon}{d\tau} - \left(\frac{\tau}{\tau_i}\right)^{-(\alpha_1+\beta)}\left[1 - \left(\frac{q_1}{q_{1Ji}}\right)\left(\frac{\tau}{\tau_i}\right)^{(2-\Gamma)\beta-\alpha_1}\right]\epsilon = 0 . \tag{7.11}$$

We examine the limiting behavior of the solutions of this equation as $\tau \to 0$. There is a critical value of the polytropic exponent $\Gamma_{cr} = 2 - \alpha_1/\beta$ which determines whether pressure is important as $\tau \to 0$. For $\Gamma < \Gamma_{cr}$ (or if the pressure is set to zero), then pressure is negligible compared to self-gravity as $\tau \to 0$, and vice versa. For $\Gamma > \Gamma_{cr}$, we define an auxiliary parameter $\delta_1 = (\Gamma - 1)\beta + 2\alpha_1$. We thus have the following cases.

i) $\Gamma < \Gamma_{cr}$, $\alpha_1 + \beta < 2$

The kinematic term dominates, and we have solutions

$$\epsilon \sim c_1\tau^{1-2\alpha_1} , \quad \epsilon \sim c_2 . \tag{7.12}$$

ii) $\Gamma < \Gamma_{cr}$, $\alpha_1 + \beta > 2$

Self-gravity dominates, and we have WKB-type growing/decaying solutions

$$\epsilon \sim c_\pm\tau^{-(3\alpha_1-\beta)/4} \exp\left[\pm\frac{B^{1/2}\tau^{-(\alpha_1+\beta-2)/2}}{(\alpha_1+\beta-2)/2}\right], \tag{7.13}$$

where $B = \tau_i^{\alpha_1+\beta}$.

iii) $\Gamma > \Gamma_{cr}$, $\delta_1 < 2$

The kinematic term dominates, so we again have the solutions

$$\epsilon \sim c_1 \tau^{1-2\alpha_1}, \quad \epsilon \sim c_2. \tag{7.14}$$

iv) $\Gamma > \Gamma_{cr}$, $\delta_1 > 2$

The pressure term dominates, and we have WKB–type oscillatory solutions:

$$\epsilon \sim c_\pm \tau^{-(\alpha_1 - \delta_1/4)} \exp\left[\pm i \frac{D^{1/2}\tau^{-(\delta_1/2-1)}}{(\delta_1/2-1)}\right], \tag{7.15}$$

where $D = (q_1/q_{1ji})\tau_i^{\delta_1}$.

We can apply these results to find the limiting behavior as $t \to t_c$ of perturbations within fluid sheets which form during the spherically symmetric or plane-symmetric collapses discussed in §§ IV and V. For a *spherical* background flow, we take $a_3 = b$. If the two-dimensional perturbation is *tangential*, then $a_1 = b$, $a_2 = a$, so that $\alpha_1 = \frac{2}{3}$, $\alpha_2 = -\frac{1}{3}$, $\beta = \frac{1}{3}$. We are interested in γ in the range $1 \le \gamma \le 5/3$, which translates to $1 \le \Gamma \le 9/5$, so that $\Gamma > \Gamma_{cr} = 0$, and $\delta_1 \le 8/5$; i.e., pressure dominates self-gravity, but kinematics in turn dominates pressure, and we have asymptotic dependences $\epsilon \propto \tau^{-1/3}$ or $\epsilon = $ constant. If the two-dimensional perturbation is *radial*, then $a_1 = a$, $a_2 = b$, so for the same range of γ, we have $\Gamma < \Gamma_{cr} = 3$, and $\alpha_1 + \beta = 0$, so self-gravity dominates pressure, but kinematics dominates both, and the limiting behaviors are $\epsilon = $ constant and $\epsilon \propto \tau^{5/3}$. For a *planar* background flow, we have $a_3 = a$ and $a_1 = a_2 = b$. But $b \to$ constant as $t \to t_c$, so that $\alpha_1 = \alpha_2 = \beta = 0$. Returning to the original equation (7.11), we find that the kinematic term vanishes, and the self-gravity and pressure terms have a constant ratio. We find that the solutions have limiting behavior $\epsilon = $ constant or $\epsilon \propto \tau$.

d) WKB Growth Factors for Pressure-free Fluid Sheet

A simple application of the results of § VII*b* is to the case that pressure is negligible within the sheet ($k \ll k_J$), and the wavevector is aligned with a principal axis, $k(t) = q_1/a_1(t)$. Then equation (7.8b) for $\omega(t)$ reduces to

$$\omega^2(t) = 2\pi G\rho_b(t)\left[\frac{2\pi a_3(t)}{q_3}\right]\left[\frac{q_1}{a_1(t)}\right] = \frac{4\pi^2 G\rho_i}{a_1^2(t)a_2(t)}\frac{q_1}{q_3}; \tag{7.16}$$

thus

$$\frac{\dot\omega}{\omega} = -\left(\frac{\dot a_1}{a_1} + \frac{1}{2}\frac{\dot a_2}{a_2}\right) \tag{7.17}$$

The factor multiplying the exponential in the WKB solution (7.9a) becomes

$$\frac{k(t)}{\sqrt{\omega(t)}} \propto \frac{a_2^{1/4}(t)}{a_1^{1/2}(t)}. \tag{7.18}$$

i) Spherical Background Flow

In this case, we have either $a_1(t) = b(t)$, $a_2(t) = a(t)$ (*tangential* perturbation) or $a_1(t) = a(t)$, $a_2(t) = b(t)$ (*radial* perturbation). The integral appearing in the exponential in the WKB solution can be written in terms of the dimensionless variables of § IV as

$$\int \omega(t)dt = \Lambda \int \frac{B(\theta)}{A_1(\theta)A_2^{1/2}(\theta)} d\theta, \tag{7.19a}$$

where

$$\Lambda \equiv (3\pi)^{1/2}\left(\frac{q_1}{q_3}\right)^{1/2}, \tag{7.19b}$$

and $A_1 \equiv (10\bar\delta_i/3)a_1$ etc. The WKB approximation is valid if $|\dot a_1/a_1\omega| \ll 1$, $|\dot a_2/a_2\omega| \ll 1$. These ratios can be written in terms of the dimensionless variables as

$$\frac{\dot a_1}{a_1\omega} = \left(\frac{1}{\Lambda}\right)\frac{A_2^{1/2}(\theta)A_1'(\theta)}{B(\theta)}, \tag{7.20a}$$

$$\frac{\dot a_2}{a_2\omega} = \left(\frac{1}{\Lambda}\right)\frac{A_1(\theta)A_2'(\theta)}{A_2^{1/2}(\theta)B(\theta)}. \tag{7.20b}$$

In Figure 8 we plot the values of $\int \omega\,dt$, $|\dot a_1/a_1\omega|$ and $|\dot a_2/a_2\omega|$, normalized to $\Lambda = 1$, as functions of θ for tangential perturbations $[A_1(\theta) = B(\theta)$, $A_2(\theta) = A(\theta)]$ for spherical collapses with $\delta_i/\bar\delta_i = (0, 0.9, 1)$. (One finds similar results for radial perturbations, but with generally smaller growth factors.) From these curves, for any given value of Λ, one can read off the approximate range of θ in which the WKB approximation is valid (once a thin sheet has formed), and also the change in the value of $\int \omega\,dt$ over any interval, which gives the exponential part of the WKB growth factor. For the generic case $\delta_i/\bar\delta_i < 1$, one finds that for any fixed $\Lambda \gg 1$, the WKB approximation is valid at early stages of the collapse, but always breaks down as $\theta \to 2\pi$, in agreement with the results of § VII*c*. For the special case $\delta_i/\bar\delta_i = 1$, WKB approximation is valid at all stages of the collapse provided $\Lambda \gg 1$.

ii) Planar Background Flow

One can perform the same analysis for a planar background flow. In this case, $a_1(t) = a_2(t) = b(t)$. In terms of the dimensionless variables used in § V, we have

$$\int \omega(t)dt = \Lambda \int \frac{d\theta}{B^{1/2}(\theta)} = \Lambda \ln \theta, \tag{7.21a}$$

where

$$\Lambda \equiv (6\pi)^{1/2}\left(\frac{q_1}{q_3}\right)^{1/2}, \tag{7.21b}$$

and

$$\frac{\dot a_1}{a_1\omega} = \frac{\dot a_2}{a_2\omega} = \frac{1}{\Lambda}\frac{B'(\theta)}{B^{1/2}(\theta)} = \frac{2}{\Lambda}. \tag{7.22}$$

We see from this that for any fixed $\Lambda \gg 1$, the WKB approximation for density perturbations in a sheet is valid at all stages of the collapse after the sheet forms. The complete WKB growth factor, including the multiplicative factor $a_2^{1/4}/a_1^{1/2} \propto 1/\theta^{1/2}$ can be written as

$$\epsilon \propto \theta^{\Lambda - 1/2}. \tag{7.23}$$

Thus the amplitude tends to a finite value as $\theta \to 1$.

VIII. SUMMARY

This paper presents an analysis of the linear evolution of short-wavelength perturbations in a background fluid flow which is undergoing gravitational collapse on large scales. The only forces acting on the fluid are assumed to be self-gravity and pressure, with a barotropic equation of state. The background flow is assumed to be non-rotating (zero vorticity). A generic flow of this type will be inhomogeneous and have a complicated velocity field, but locally, in the neighborhood of a point comoving with the fluid, it looks like a piece of a homogeneous, anisotropic flow having a linear velocity field, and described by a matrix of scale factors $A_{ij}(t)$. The local evolution
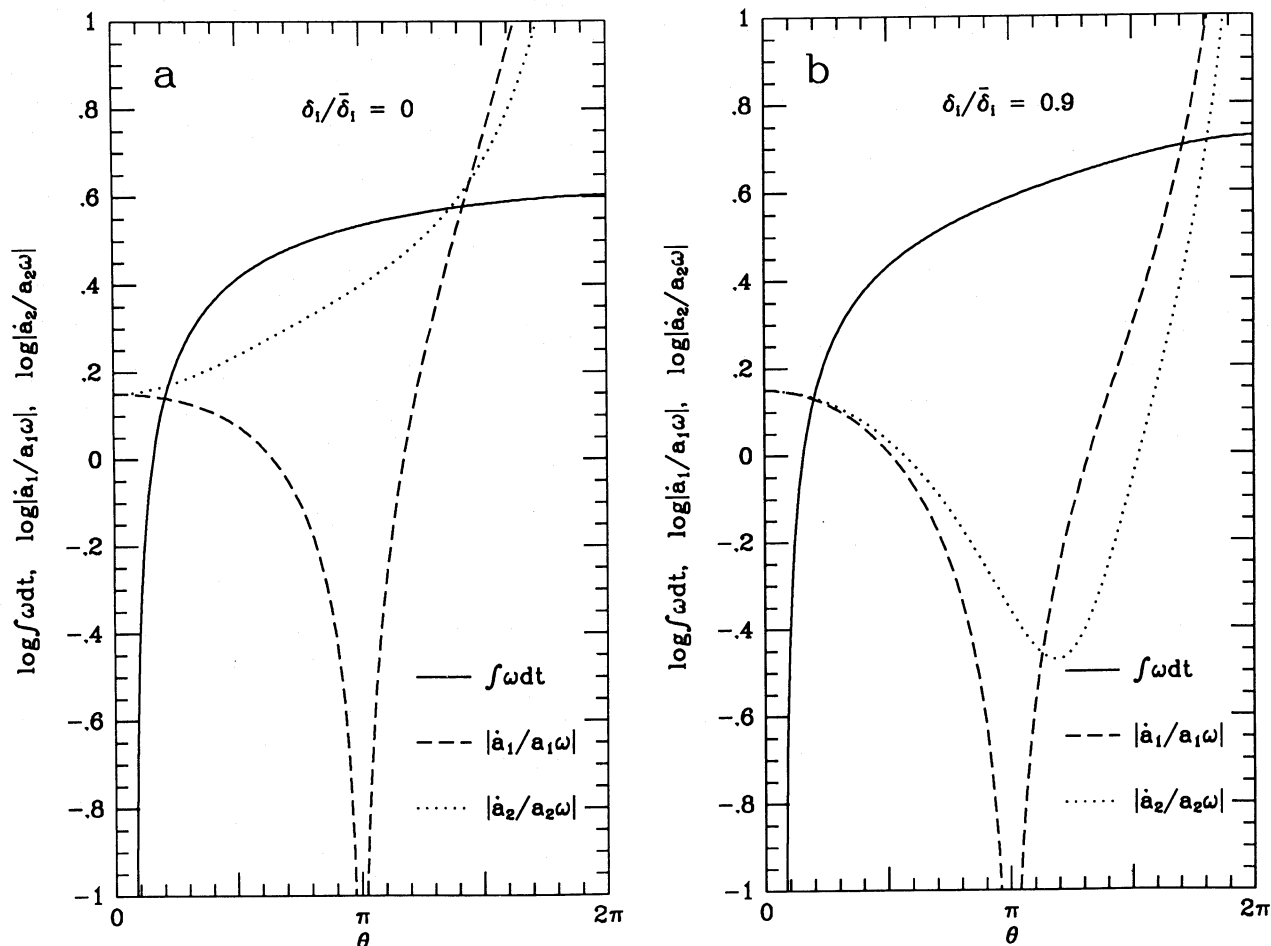
FIG. 8.—WKB growth factor for tangential perturbation in thin sheet formed in spherical background flow (see text for details). Plotted are $\int \omega \, dt$, $|\dot{a}_1/a_1\omega|$, and $|\dot{a}_2/a_2\omega|$. (a) $\delta_i/\bar{\delta}_i = 0$. (b) $\delta_i/\bar{\delta}_i = 0.9$. (c) $\delta_i/\bar{\delta}_i = 1$.

of perturbations in the short-wavelength limit in an inhomogeneous flow is the same as that in the equivalent homogeneous flow, the effects of large-scale gradients entering only through the scale factors $A_{ij}(t)$. In § II, I derive the evolution equations for locally plane-wave perturbations with wavevector **k**. The existence of a conserved vorticity variable (with two independent components) allows the system of equations to be reduced from fourth-order to second-order in time. One finds four independent perturbation modes: two of these have vorticity and the other two are vorticity-free, with purely longitudinal peculiar velocities. Specializing to a flow in which the principal axes of the local shear are fixed in time, the matrix $A_{ij}(t)$ is diagonalized, with components $a_i(t)$ along these principal axes. The anisotropy of the local velocity field then causes the wavevector of a perturbation to be sheared toward alignment with the principal axis having the smallest scale factor $a_i(t)$, unless the wavevector happens to be exactly aligned with one of the other principal axes. As a result of this shear, vorticity and density perturbations are coupled: a vorticity perturbation in general drives the growth of a density perturbation.

Aside from vorticity, the evolution of the density perturbation ϵ depends on pressure (represented by a term $c_s^2 k^2$), self-gravity (a term $4\pi G\rho$), and the kinematics of the background flow (represented by a term depending on the expansion rates $\dot{a}_i/a_i$ and on the orientation of the wavevector). The

pressure term tends to cause oscillations in ϵ (sound waves), while the self-gravity term tends to cause ϵ to grow. The kinematic term either damps or amplifies the peculiar velocity parallel to a principal axis according as there is expansion ($\dot{a}_i/a_i > 0$) or contraction ($\dot{a}_i/a_i < 0$) along that axis, thus hindering or helping growth in ϵ. Pressure and self-gravity balance at the Jeans wavenumber $k_J = (4\pi G\rho)^{1/2}/c_s$. If $k \ll k_J$, pressure is negligible and ϵ grows at a rate independent of the magnitude of the wavevector **k**. However, the kinematic effect may dominate over self-gravity in driving perturbation growth, and may drive growth even when pressure dominates self-gravity. Growth in ϵ driven by kinematics depends on the direction of the wavevector—it is fastest when the wavevector is aligned with the fastest contracting principal axis.

For the specific background collapses studied in this paper, which are pressure-free and start from nearly homogeneous and isotropic initial conditions, the effect of background kinematics on perturbation growth is initially comparable to that of self-gravity, but it comes to dominate as the collapse proceeds and gravitational tidal fields cause the local velocity field around any point to become increasingly anisotropic. For spherically symmetric background flows, the growth in anisotropy results from the increasing inhomogeneity (central concentration) of the density distribution, while for plane-symmetric flows it results from the increasing flattening. For a
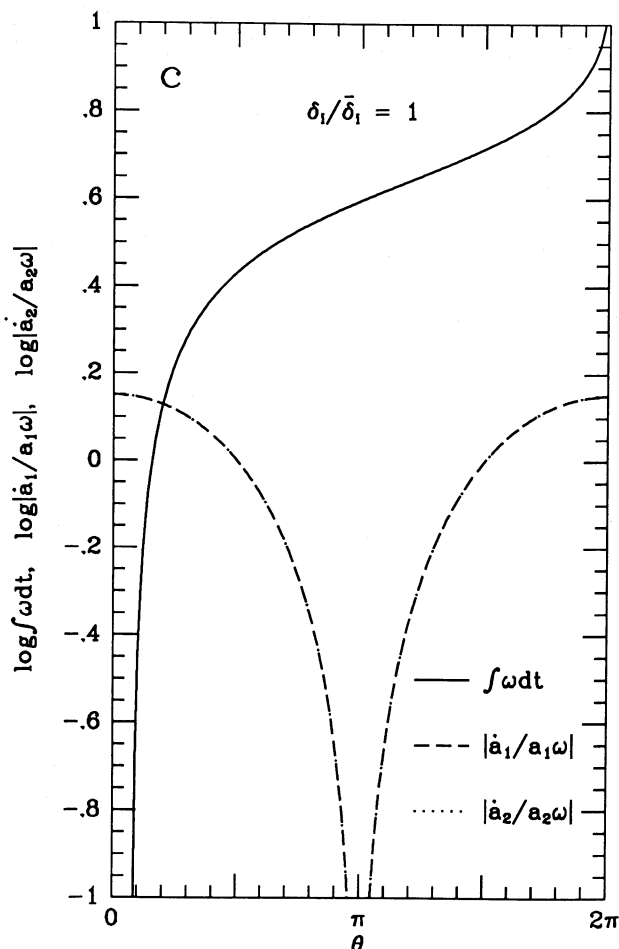
FIG. 8—Continued

given for the case of negligible pressure ($k \ll k_J$). Perturbation evolution is sensitive to the orientation of the wavevector, which tends to get sheared toward being tangential. Growth of density is fastest when the wavevector is tangential, and is dominated by kinematics rather than self-gravity in the late stages. At late times, the density perturbation generically varies as $\epsilon \propto (t_c - t)^{-1/3}$, t_c being the collapse time, in contrast to the behavior found for collapse of a uniform sphere ($\delta_i/\bar{\delta}_i = 1$), which is $\epsilon \propto (t_c - t)^{-1}$.

For a plane-symmetric background flow, as discussed in § V, the local properties of the background solution are (after scaling) completely specified, with no adjustable parameters. The local flow becomes anisotropic in the sense that at late stages there is contraction along the collapse axis perpendicular to the symmetry plane, and expansion along two degenerate principal axes in the tangential directions. The classification of the four perturbation modes is the same as for the spherical case. The wavevector of a perturbation tends to be sheared toward the collapse direction, and the growth of ϵ is fastest for this orientation. At late times, the growth of density perturbations (for zero pressure) is dominated by kinematics rather than self-gravity, with the dependence. $\epsilon \propto (t_c - t)^{-1}$.

For a generic collapse which is neither homogeneous nor spherical, it seems likely that during the later stages, growth of density perturbations will be dominated by the background kinematics rather than self-gravity. In general, there will be a single fastest contracting principal axis, and perturbation growth will be fastest when the wavevector is aligned with this axis. Therefore, as discussed in § VI, the nonlinear development of these perturbations is likely to lead to collapse to planar structures ("pancakes") oriented perpendicular to the preferred axis. (In the special case that the two fastest contracting axes are degenerate, as for a spherical background flow, the collapse is likely to be planar in the first instance, but with the planes later collapsing down to filaments aligned along the slowest contracting axis.) For a collisional fluid, the resulting planar gas layer may reach vertical equilibrium while it is still nearly comoving with the background flow in the transverse directions, under the influence of the background tidal forces, and be quite thin relative to its transverse extent if the collapse is accompanied by sufficient energy dissipation. Section VII considers perturbation growth in a thin fluid sheet undergoing shearing motion, which is essentially the two-dimensional analog of the three-dimensional problem discussed in the previous sections. A distinctive feature of the two-dimensional problem is that the self-gravity of a perturbation increases with increasing wavenumber. Provided the sound speed in the sheet is small enough, there is a range of wavelengths, between the large scales on which kinematics dominate and the small scales on which pressure dominates, over which self-gravity causes perturbations to grow much more rapidly than would perturbations of the same wavelength which were still part of the three-dimensional background flow.

The results of this paper suggest the following scenario for the fragmentation of a cold collapsing flow. If the collapse starts from nearly homogeneous and isotropic initial conditions, then initially self-gravity contributes significantly to growth of density perturbations, and perturbations which go nonlinear at this stage will collapse to self-gravitating objects. At later stages, the collapse becomes anisotropic as tidal fields grow, and the mechanism of perturbation growth becomes mainly kinematic. Perturbations which go nonlinear at this stage collapse to planar pancakes which may not be self-

generic collapse, both of these mechanisms are likely to operate to some extent. It seems likely that the result that background kinematics come to dominate over self-gravity will be a fairly general one for collapses in which pressure is unimportant on large scales.

Perturbation evolution is studied in detail for background flows having either spherical symmetry or planar symmetry (no symmetry is imposed on the perturbations). In both cases, the initial conditions are taken to be linear perturbations of an $\Omega = 1$ cosmological model, and pressure is assumed to be negligible on the scale of the background flow (although it may still be important on small scales). With these assumptions, the nonlinear evolution of the background flow can be derived analytically up to the time that mass shells cross. For spherical flows, discussed in § IV, the local properties of the background flow about any comoving point can, after suitable scaling, be specified by a single parameter $\delta_i/\bar{\delta}_i$, the initial ratio of the overdensity on a spherical shell to the mean interior overdensity. In the generic case $\delta_i/\bar{\delta}_i < 1$ of a perturbation with some degree of central concentration, the local flow becomes anisotropic in the sense that there is at late stages contraction along two degenerate principal axes in the tangential directions, and expansion along the radial direction. Of the perturbation modes, one is a vorticity mode with velocity transverse to the wavevector at all times, another has both transverse and longitudinal velocity components, and the other two are purely longitudinal (vorticity-free). Detailed results for the modes are

gravitating. However, these pancakes, if gaseous, may be susceptible to self-gravitating instabilities on small scales, leading to formation of gravitationally bound fragments. The characteristic sizes of the fragments formed by this two stage process will be sensitive to the amount of radiative cooling in the pancake. Clearly, the scenario outlined requires further investigation. However, if correct it could have important implications for galaxy formation and star formation.

APPENDIX A

RELATION OF TWO-DIMENSIONAL AND THREE-DIMENSIONAL POLYTROPIC COEFFICIENTS

We consider a fluid sheet with planar symmetry which in the perpendicular (z) direction is self-gravitating and in hydrostatic equilibrium. The three-dimensional pressure $p(z)$, volume density $\rho(z)$, and gravitational potential $\Phi(z)$ are related by

$$\frac{dp}{dz} = -\rho \frac{d\Phi}{dz} , \tag{A1a}$$

$$\frac{d^2\Phi}{dz^2} = 4\pi G\rho . \tag{A1b}$$

With the polytropic relation $p = \kappa\rho^\gamma$, these can be combined into a single equation:

$$\frac{d}{dz}\left(\kappa\gamma\rho^{\gamma-2}\frac{d\rho}{dz}\right) + 4\pi G\rho = 0 . \tag{A2}$$

The method of solution of this equation is given by Goldreich and Lynden-Bell (1965) as follows. Define $\rho_c = \rho(z = 0)$. Then

$$\left(\frac{\rho}{\rho_c}\right)^\gamma = \cos^2 X , \tag{A3a}$$

where $X(z)$ is given implicitly by integrating

$$\frac{dz}{dX} = \left(\frac{\kappa\rho_c^{\gamma-2}}{2\pi G}\right)^{1/2}(\cos X)^{1-2/\gamma} . \tag{A3b}$$

The surface density σ is then given by

$$\sigma = 2\int_0^\infty \rho(z)dz = 2\int_0^{\pi/2}\rho(X)\left(\frac{dz}{dX}\right)dX = \left(\frac{2\kappa\rho_c^\gamma}{\pi G}\right)^{1/2} , \tag{A4}$$

while the vertically integrated pressure P is given by

$$P = 2\int_0^\infty p(z)dz = 2\int_0^{\pi/2}\kappa\rho^\gamma(X)\left(\frac{dz}{dX}\right)dX = \left(\frac{2\kappa^3\rho_c^{3\gamma-2}}{\pi G}\right)^{1/2}I_\gamma , \tag{A5a}$$

where

$$I_\gamma = 2^{2(1-1/\gamma)}B(2 - 1/\gamma, 2 - 1/\gamma) , \tag{A5b}$$

and $B(x, y)$ is the beta function. The quantity I_γ is finite for $\gamma > \frac{1}{2}$. Particular values are $I_1 = 1$ and $I_2 = \pi/4$. Combining equations (A4) and (A5), we obtain a polytropic relation between the two-dimensional pressure P and the surface density σ:

$$P = K\sigma^\Gamma , \tag{A6a}$$

where

$$\Gamma = 3 - 2/\gamma , \tag{A6b}$$

$$K = \left(\frac{\pi G}{2}\right)^{1-1/\gamma}\kappa^{1/\gamma}I_\gamma , \tag{A6c}$$

If we define the effective thickness of the fluid sheet by $h \equiv \sigma/2\rho_c$, then it follows from combining the above equations that

$$h = \frac{C_s^2}{\Gamma I_\gamma \pi G\sigma} , \tag{A7}$$

where $C_s = (dP/d\sigma)^{1/2}$ is the two-dimensional sound speed.

APPENDIX B

WKB SOLUTIONS

We consider the solutions of an equation of the form

$$\frac{d^2y}{dx^2} + a(x)\frac{dy}{dx} = \frac{1}{\epsilon^2} Q(x)y , \tag{B1}$$

in the limit $\epsilon \to 0$. We define new variables

$$z(x) = \int^x \frac{dx'}{\exp\left[\int^{x'} a(x'')dx''\right]} , \qquad q(z) = \exp\left[2\int^x a(x')dx'\right]Q(x) , \tag{B2}$$

in terms of which equation (B1) becomes

$$\frac{d^2y}{dz^2} = \frac{1}{\epsilon^2} q(z)y . \tag{B3}$$

This equation is of standard Shrödinger form. The solutions as $\epsilon \to 0$ are (e.g., Bender and Orszag 1978, § 10.1)

$$y(z) \sim \frac{c_\pm}{|q(z)|^{1/4}} \exp\left[\pm\frac{1}{\epsilon}\int^z \sqrt{q(t)}dt\right] , \tag{B4a}$$

and the condition for this to be a good approximation is, roughly,

$$\epsilon\left|\frac{dq/dz}{q^{3/2}(z)}\right| \ll 1 \tag{B4b}$$

(Bender and Orszag give a more precise criterion). Transforming back to the original variables, we obtain the solutions

$$y(x) \sim \frac{c_\pm}{|Q(x)|^{1/4}} \exp\left[\pm\frac{1}{\epsilon}\int^x \sqrt{Q(t)}dt - \frac{1}{2}\int^x a(t)dt\right] , \tag{B5a}$$

with the conditions for this to be a good approximation being roughly

$$\epsilon\left|\frac{Q'(x)}{Q^{3/2}(x)}\right| \ll 1 , \qquad \epsilon\left|\frac{a(x)}{Q^{1/2}(x)}\right| \ll 1 . \tag{B5b}$$

This transformation of variables can also be used to derive the connection formulae relating the WKB solutions on either side of a point $x = x_0$ at which $Q(x_0) = 0$ to those for an equation of the standard form (B3), if these are needed.

REFERENCES

Aarseth, S. J., Lin, D. N. C., and Papaloizou, J. C. B. 1988, *Ap. J.*, **324**, 288.
Arny, T. T. 1966, *Ap. J.*, **145**, 572.
———. 1967, *Ann. d'Ap.*, **30**, 1.
Balbus, S. A. 1988a, *Ap. J.*, **324**, 60.
———. 1988b, *Ap. J.*, **328**, 395.
Bender, C. M., and Orszag, S. A. 1978, *Advanced Mathematical Methods for Scientists and Engineers* (New York: McGraw-Hill).
Blumenthal, G. R., Faber, S. M., Primack, J. R., and Rees, M. J. 1984, *Nature*, **311**, 517.
Falle, S. A. E. G. 1972, *M.N.R.A.S.*, **156**, 265.
Goldreich, P., and Lynden-Bell, D. 1965, *M.N.R.A.S.*, **130**, 125.
Goodman, J., and Binney, J. 1983, *M.N.R.A.S.*, **203**, 265.
Hunter, C. 1962, *Ap. J.*, **135**, 594.
———. 1964, *Ap. J.*, **139**, 570.
———. 1983, in *Fluid Dynamics in Astrophysics and Geophysics*, ed. N. R. Lebovitz (New York: American Mathematical Society), p. 179.
Larson, R. B. 1985, *M.N.R.A.S.*, **214**, 379.

Lifshitz, E. M. 1946, *J. Phys. (USSR)*, **10**, 118.
Lin, C. C., Mestel, L., and Shu, F. H. 1965, *Ap. J.*, **142**, 1431.
Lynden-Bell, D. 1967, *M.N.R.A.S.*, **136**, 101.
McNally, D., and Settle, J. J. 1980, *M.N.R.A.S.*, **192**, 917.
Peebles, P. J. E. 1980, *The Large-Scale Structure of the Universe* (Princeton: Princeton University Press).
Ryden, B. S., and Gunn, J. E. 1987, *Ap. J.*, **318**, 15.
Silk, J. 1982, *Ap. J.*, **256**, 514.
Silk, J., and Suto, Y. 1988, *Ap. J.*, **335**, 295.
Tohline, J. E. 1982, *Fund. Cosmic Phys.*, **8**, 1.
Tomisaka, K., and Ikeuchi, S. 1985, *Pub. Astr. Soc. Japan*, **37**, 461.
Weinberg, S. 1972, *Gravitation and Cosmology* (New York: Wiley).
Zel'dovich, Ya. B. 1970, *Astrophysics*, **6**, 164.
Zel'dovich, Ya. B., and Kazhdan, Ya. M. 1970, *Astrophysics*, **6**, 50.
Zel'dovich, Ya. B., and Novikov, I. D. 1983, *Relativistic Astrophysics*, Vol. **2**, *The Structure and Evolution of the Universe* (Chicago: University of Chicago Press).

CEDRIC G. LACEY: Astronomy Department, University of California, Berkeley, CA   94720